Contribution from the Department of Chemistry and Biochemistry, University of California, Los Angeles, California 90024-1569

Coordination of "Noncoordinating" Anions: Synthesis, Characterization, and X-ray Crystal Structures of Fluorine-Bridged $[SbF_6]^-$, $[BF_4]^-$, and $[PF_6]^-$ Adducts of $[R_3P(CO)_3(NO)W]^+$. An Unconventional Order of Anion Donor Strength

Robert V. Honeychuck and William H. Hersh*

Received February 24, 1989

The syntheses of *mer*-(*cis*-L)(*trans*-NO)$(CO)_3$W(μ-F)EF_n [EF_n = SbF_5, L = Me_3P (**3a**), Me_2PhP (**3b**), Cy_3P (Cy = cyclohexyl, **3c**); EF_n = BF_3, L = Me_3P (**5**); EF_n = PF_5; L = Me_3P (**6**)] from $LW(CO)_5$ and $[NO][EF_{n+1}]$ are described. The $[SbF_6]^-$ adducts are reasonably stable at room temperature, the $[BF_4]^-$ adduct qualitatively less so, and the $[PF_6]^-$ adduct decomposes within 2 days at room temperature. Neutral donor ligands including phosphines, acetonitrile, aldehydes, and ketones immediately displace the anion to give [*mer*-(*cis*-Me_3P)(*trans*-NO)$(CO)_3$WL][EF_{n+1}]. Cotton–Kraihanzel force constants are calculated for each of the fully characterized compounds. The ^{13}C, ^{19}F, and ^{31}P NMR spectra of **3**, **5**, and **6** confirm that the noncoordinating anions are bound to tungsten via a bridging fluorine atom in CD_2Cl_2 solution. At 185 K, the ^{19}F NMR spectra of **5** and **6** exhibit well-separated peaks for the bridging and terminal fluorine atoms, and in the latter case for **6** these are further separated into signals for the equatorial and axial fluorine atoms. The ^{31}P NMR spectra of **3a**, **5**, and **6** each exhibit a doublet below 195 K due to coupling of the bridging fluorine atom and the cis-Me_3P phosphorus atom; upon warming, **3a** and **6** each exhibit a septet due to anion "spinning" in which each of the six fluorine atoms of the $[SbF_6]^-$ and $[PF_6]^-$ ligands exchanges into the bridging site, while **5** exhibits a quintet due to exchange of the four fluorine atoms of the $[BF_4]^-$ ligand. The phosphate phosphorus atom of **6** exhibits a sharp sextet of doublets at 165 K due to different bridging and terminal fluorine coupling constants. Above room temperature, coalescence to a broad singlet occurs for the Me_3P phosphorus atoms of **3a**, **5**, and **6** due to fast intermolecular exchange. The structures of **3b**, **3c**, **5**, and **6** have been confirmed by X-ray crystallography, and they comprise the first set of essentially isostructural adducts of $[SbF_6]^-$, $[BF_4]^-$, and $[PF_6]^-$. Crystallographic data for **3b**: space group $P2_1/n$, a = 8.838 (3) Å, b = 8.267 (2) Å, c = 25.004 (7) Å, β = 94.71 (1)°, Z = 4, R = 0.056. Data for **3c**: space group $P\bar{1}$, a = 9.925 (2) Å, b = 10.604 (2) Å, c = 14.010 (2) Å, α = 84.088 (3)°, β = 70.390 (3)°, γ = 81.051 (4)°, Z = 2, R = 0.026. Data for **5**: space group $P2_1/n$, a = 6.709 (1) Å, b = 12.249 (2) Å, c = 16.457 (3) Å, β = 98.352 (7)°, Z = 4, R = 0.047. Data for **6**: space group $P2_1/n$, a = 7.424 (2) Å, b = 21.207 (6) Å, c = 9.089 (2) Å, β = 99.220 (7)°, Z = 4, R = 0.061. The W–(μ-F) and (μ-F)–E (E = Sb, B, P) bond lengths are 2.169 (11) and 1.954 (11) Å (**3b**), 2.186 (3) and 1.979 (3) Å (**3c**), 2.168 (7) and 1.500 (14) Å (**5**), and 2.187 (10) and 1.733 (11) Å (**6**). Bond length comparisons are made with 16 other adducts of $[SbF_6]^-$, $[BF_4]^-$, $[PF_6]^-$, and $[ReF_6]^-$, and an absolute scale of anion E–(μ-F) bond length distortion, D_d°, is proposed. We suggest that the $[BF_4]^-$ and $[PF_6]^-$ adducts **5** and **6** exhibit the maximum degree of distortion that is possible without cleaving the B–(μ-F) or P–(μ-F) bond, while in the $[SbF_6]^-$ adducts **3b** and **3c** the Sb–(μ-F) bond is lengthened only to 40–60% of the maximum degree of distortion possible. We conclude that the order of ligand binding strength is $[SbF_6]^- > [BF_4]^- > [PF_6]^-$.

Introduction

Homogeneous catalysis by stable transition-metal complexes is a contradiction in terms. A requirement for catalysis is the availability of free coordination sites on the metal, yet stability—as loosely defined in a practical sense by one's ability to isolate the catalyst—typically depends on coordinative and electronic saturation. Thus, routes to discovery of new catalysts might include the preparation of unsaturated compounds that are somehow stable or of saturated compounds that possess labile ligands that will offer only weak competition with substrate molecules for the metal coordination sites.[1] In cationic complexes, which are the present focus of our attention, an anionic counterion must always be present, and hence it must of necessity be "noncoordinating". What is meant, of course, is that it be only weakly coordinating,[2] since coordination complexes of so-called noncoordinating anions such as $[RSO_3]^-$ (R = F, CF_3),[3] $[XO_4]^-$ (X = Cl, Re),[4] $[BF_4]^-$,[3b,4k,5] $[PF_6]^-$,[4k,5i-l,6] and $[AsF_6]^-$[5k,s,7] have been known for years, and in fact the search for new noncoordinating anions is an active area of research.[8] Chemical characterization of these materials typically has rested on elemental analysis, the apparently facile displacement of these anions by relatively weakly donating neutral ligands to give more tractable cationic complexes, and infrared analysis of bands due to the anionic fragment. In addition, X-ray crystal structures revealing coordinated $[CF_3SO_3]^-$, $[ClO_4]^-$, and $[BF_4]^-$ have been reported.[3b,c,4a-c,5a-h]

On the basis of much comparative work,[3-7,9] the order of decreasing donor ability of the noncoordinating anions is arguably that in which they are listed above. Notably absent from this list is $[SbF_6]^-$, which might be considered to be the worst coordinating of the simple noncoordinating anions on the basis of the assumption that anion donor ability should exhibit an inverse correlation with

(1) See for instance: (a) Burch, R. R.; Shusterman, A. J.; Muetterties, E. L.; Teller, R. G.; Williams, J. M. *J. Am. Chem. Soc.* **1983**, *105*, 3546–3556. (b) Wasserman, H. J.; Kubas, G. J.; Ryan, R. R. *Ibid.* **1986**, *108*, 2294–2301. (c) Werner, H.; Esteruelas, M. A.; Otto, H. *Organometallics* **1986**, *5*, 2295–2299. (d) Crabtree, R. H.; Faller, J. W.; Mellea, M. F.; Quirk, J. M. *Ibid.* **1982**, *1*, 1361–1366. (e) Burk, M. J.; Crabtree, R. H.; Holt, E. M. *Ibid.* **1984**, *3*, 638–640. (f) Cotton, F. A.; Lahuerta, P.; Sanau, M.; Schwotzer, W.; Solana, I. *Inorg. Chem.* **1986**, *25*, 3526–3528. (g) Crabtree, R. H. *Chem. Rev.* **1985**, *85*, 245–269.

(2) (a) Rosenthal, M. R. *J. Chem. Educ.* **1973**, *50*, 331–335. (b) For a comprehensive review, see: Beck, W.; Sünkel, K. *Chem. Rev.* **1988**, *88*, 1405–1421.

(3) (a) Trogler, W. C. *J. Am. Chem. Soc.* **1979**, *101*, 6459–6460. (b) Olgemöler, B.; Bauer, H.; Löbermann, H.; Nagel, U.; Beck, W. *Chem. Ber.* **1982**, *115*, 2271–2286. (c) Humphrey, M. B.; Lamanna, W. M.; Brookhart, M.; Husk, G. R. *Inorg. Chem.* **1983**, *22*, 3355–3358. (d) Merrifield, J. H.; Fernández, J. M.; Buhro, W. E.; Gladysz, J. A. *Ibid.* **1984**, *23*, 4022–4029. (e) Nitschke, J.; Schmidt, S. P.; Trogler, W. C. *Ibid.* **1985**, *24*, 1972–1978. (f) Lawrance, G. A. *Chem. Rev.* **1986**, *86*, 17–33. (g) Appel, M.; Schloter, K.; Heidrich, J.; Beck, W. *J. Organomet. Chem.* **1987**, *322*, 77–88. (h) Ferrara, J. D.; Tessier-Youngs, C.; Youngs, W. J. *Organometallics* **1987**, *6*, 676–678.

(4) (a) Reed, C. A.; Mashiko, T.; Bentley, S. P.; Kastner, M. E.; Scheidt, W. R.; Spartalian, K.; Lang, G. *J. Am. Chem. Soc.* **1979**, *101*, 2948–2958. (b) Foley, J.; Kennefick, D.; Phelan, D.; Tyagi, S.; Hathaway, B. *J. Chem. Soc., Dalton Trans.* **1983**, 2333–2338. (c) House, D. A.; Steel, P. J.; Watson, A. A. *J. Chem. Soc., Chem. Commun.* **1987**, 1575–1576. (d) Hathaway, B. J.; Underhill, A. E. *J. Chem. Soc.* **1961**, 3091–3096. (e) Brown, D. H.; Nuttall, R. H.; McAvoy, J.; Sharp, D. W. A. *J. Chem. Soc. A* **1966**, 892–896. (f) Usón, R.; Riera, V.; Gimeno, J.; Laguna, M.; Gamasa, M. P. *J. Chem. Soc., Dalton Trans.* **1979**, 996–1002. (g) Peone, J., Jr.; Vaska, L. *Angew. Chem., Int. Ed. Engl.* **1971**, *10*, 511–512. (h) Wimmer, F. L.; Snow, M. R. *Aust. J. Chem.* **1978**, *31*, 267–278. (i) Lenz, E.; Murmann, R. K. *Inorg. Chem.* **1968**, *7*, 1880–1885. (j) Mayfield, H. G., Jr.; Bull, W. E. *Inorg. Chim. Acta* **1969**, *3*, 676–680. (k) Isobe, K.; Nanjo, K.; Nakamura, Y.; Kawaguchi, S. *Chem. Lett.* **1979**, 1193–1196. (l) Gowda, N. M. N.; Naikar, S. B.; Reddy, G. K. N. *Adv. Inorg. Chem. Radiochem.* **1984**, *28*, 255–299. (m) Heidrich, J.; Loderer, D.; Beck, W. *J. Organomet. Chem.* **1986**, *312*, 329–333. (n) Hillhouse, G. L.; Haymore, B. L. *Inorg. Chem.* **1987**, *26*, 1876–1885.

0020-1669/89/1328-2869$01.50/0

acid strength. The HF/SbF_5 system *is* apparently the strongest known acid;[10] on one scale, it has a pK_a of 0, compared to 2.1, 6.6, and 9.5 for the AsF_5, BF_3, and PF_5 systems, respectively.[10c] This acidity is well documented by the body of work on characterization of carbocations in superacid media,[11] since unlike SbF_5 (as well as AsF_5), BF_3 and PF_5 are not sufficiently powerful Lewis acids to yield carbocations and $[BF_4]^-$ or $[PF_6]^-$ by fluoride abstraction from an alkyl fluoride.[11a,b] As far as carbon Lewis acids are concerned, $[SbF_6]^-$ *can* be a truly noncoordinating anion, as seen in the reaction of *tert*-butyl fluoride in the $SbF_5/HSO_3F/SO_2$ ("magic acid") solvent system, which yields the fully ionized *tert*-butyl carbocation in the presence of $[SbF_6]^-$ as the major counterion.[11d] Nonetheless, covalent adducts of $[SbF_6]^-$ *are* known, the most common being that with SbF_5 to give $[Sb_2F_{11}]^-$ (**1**).[11c,d,12]

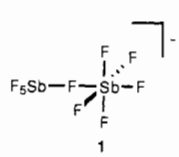

1

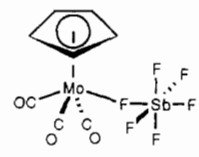

2

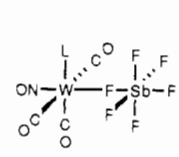

3a L = Me_3P
3b L = Me_2PhP
3c L = Cy_3P

For instance, reaction of *tert*-butyl fluoride with neat SbF_5 yields $[Sb_2F_{11}]^-$ rather than $[SbF_6]^-$ as the simplest anion,[11c] and cations such as $[CH_3]^+$ and $[Me_3Sn]^+$ also bind $[SbF_6]^-$, giving CH_3–F–SbF_5 and Me_3Sn–F–SbF_5.[11g,13] More recently, uranium and transition-metal adducts have been reported, in which the high-oxidation-state oxide and oxyfluoride fragments $[UO_2]^{2+}$, $[UF_2O]^{2+}$, and $[MF_3O]^+$ (M = Mo, W, Re) bind $[SbF_6]^-$, to give $[O_2U(\mu\text{-}F)SbF_5][\eta^2\text{-}Sb_2F_{11}]$, $OF_2U\{(\mu\text{-}F)SbF_5\}_2$, and $\{OF_3M(\mu\text{-}F)SbF_5\}_n$ (M = Mo, $n = \infty$; M = Re, $n = 2$),[14] each of which is again structurally related to $[Sb_2F_{11}]^-$. While these materials are formally coordination complexes of $[SbF_6]^-$, their chemistry—such as their synthesis from metal fluorides and SbF_5—is rather different from the $[RSO_3]^-$, $[XO_4]^-$, $[BF_4]^-$, $[PF_6]^-$, and $[AsF_6]^-$ adducts referred to above.[2b,3-7] The first *low*-oxidation-state transition-metal adduct of $[SbF_6]^-$, $Cp(CO)_3Mo(\mu\text{-}F)SbF_5$ (**2**), was described by Beck in 1983, and the report included an elemental analysis, IR and ^1H NMR spectra, and reactions with $Cp(CO)_2FeC(O)Me$ and Cp_2Ni.[7b] We recently reported the novel synthesis of two tungsten nitrosyl adducts of $[SbF_6]^-$, $L(CO)_3(NO)W(\mu\text{-}F)SbF_5$ (L = Me_3P (**3a**), Me_2PhP (**3b**)), including the first X-ray crystal structure of a low-oxidation-state adduct of $[SbF_6]^-$ and definitive NMR evidence that the solid-state $[SbF_6]^-$ coordination persists in solution.[15] More recent reports of $[SbF_6]^-$ coordination to transition metals[5k,16] have included an X-ray diffraction study of an iron porphinato complex[16a] and a ^{19}F NMR study that revealed solution coordination of $[SbF_6]^-$ (as well as $[AsF_6]^-$).[16b]

Taken together, the work described above might suggest that the relative rarity of low-oxidation-state transition-metal adducts of $[SbF_6]^-$ may be due merely to its *assumed* lack of donor ability toward metals, in which the conventional wisdom is that $[SbF_6]^-$ adducts are less stable than $[BF_4]^-$ and $[PF_6]^-$ adducts. In order to examine the validity of this assumption, we have undertaken a physical study of essentially isostructural transition-metal adducts of $[SbF_6]^-$, $[BF_4]^-$, and $[PF_6]^-$, in which the goal is the direct comparison of these materials both in the solid state and in solution. In this paper we report the syntheses and characterization of these compounds and the first *set* of X-ray crystal structures of related adducts of the noncoordinating anions $[SbF_6]^-$, $[BF_4]^-$, and $[PF_6]^-$. Perhaps surprisingly, given the long history of such compounds, the $[PF_6]^-$ structure is the first of its kind. In a future paper we will describe and compare the dynamic solution structures of these $[SbF_6]^-$, $[BF_4]^-$, and $[PF_6]^-$ adducts.[17]

Results

Synthesis and Initial Chemical Characterization. Addition of a single equivalent of solid $[NO][SbF_6]$ to a stirred CH_2Cl_2 solution of $LW(CO)_5$ (L = Me_3P, Et_3P, *n*-oct_3P, Me_2PhP, $MePh_2P$, Cy_3P) resulted in rapid bubbling and immediate formation of an orange solution, as the $[NO][SbF_6]$ dissolved. Infrared analysis upon cessation of bubbling, usually 15–30 min, typically showed fairly complete consumption of starting material,

(5) (a) Brown, D. S.; Lee, J. D.; Melsom, B. G. A.; Hathaway, B. J.; Procter, I. M.; Tomlinson, A. A. G. *J. Chem. Soc., Chem. Commun.* **1967**, 369–371. (b) Tomlinson, A. A. G.; Bonamico, M.; Dessy, G.; Fares, V.; Scaramuzza, L. *J. Chem. Soc., Dalton Trans.* **1972**, 1671–1674. (c) Gaughan, A. P., Jr.; Dori, Z.; Ibers, J. A. *Inorg. Chem.* **1974**, *13*, 1657–1667. (d) Kindberg, B. L.; Griffith, E. H.; Amma, E. L. *J. Chem. Soc., Chem. Commun.* **1977**, 461–462. (e) Baker, E. N.; Norris, G. E. *J. Chem. Soc., Dalton Trans.* **1977**, 877–882. (f) Nakai, H. *Bull. Chem. Soc. Jpn.* **1983**, *56*, 1637–1641. (g) Velthuizen, W. C.; Haasnoot, J. G.; Kinneging, A. J.; Rietmeijer, F. J.; Reedijk, J. *J. Chem. Soc., Chem. Commun.* **1983**, 1366–1368. (h) Hitchcock, P. B.; Lappert, M. F.; Taylor, R. G. *Ibid.* **1984**, 1082–1084. (i) Beck, W.; Schloter, K. *Z. Naturforsch., B* **1978**, *33B*, 1214–1222. (j) Sünkel, K.; Urban, G.; Beck, W. *J. Organomet. Chem.* **1983**, *252*, 187–194. (k) Sünkel, K.; Urban, G.; Beck, W. *Ibid.* **1985**, *290*, 231–240. (l) Fernández, J. M.; Gladysz, J. A. *Inorg. Chem.* **1986**, *25*, 2672–2674. (m) Vallarino, L. M.; Hill, W. E.; Quagliano, J. V. *Ibid.* **1965**, *4*, 1598–1604. (n) Legzdins, P.; Mitchell, R. W.; Rempel, G. L.; Ruddick, J. D.; Wilkinson, G. *J. Chem. Soc. A* **1970**, 3322–3326. (o) Richter, K.; Fischer, E. O.; Kreiter, C. G. *J. Organomet. Chem.* **1976**, *122*, 187–196. (p) Fischer, E. O.; Walz, S.; Ruhs, A.; Kreissl, F. R. *Chem. Ber.* **1978**, *111*, 2765–2773. (q) Raab, K.; Olgemoller, B.; Schloter, K.; Beck, W. *J. Organomet. Chem.* **1981**, *214*, 81–86. (r) Mattson, B. M.; Graham, W. A. G. *Inorg. Chem.* **1981**, *20*, 3186–3189. (s) Raab, K.; Nagel, U.; Beck, W. *Z. Naturforsch., B* **1983**, *38B*, 1466–1476. (t) Legzdins, P.; Martin, D. T. *Organometallics* **1983**, *2*, 1785–1791. (u) Horn, E.; Snow, M. R. *Aust. J. Chem.* **1984**, *37*, 1375–1393. (v) Bauer, H.; Beck, W. *J. Organomet. Chem.* **1986**, *308*, 73–83. (w) Thomas, R. R.; Chebolu, V.; Sen, A. *J. Am. Chem. Soc.* **1986**, *108*, 4096–4103. (x) Appel, M.; Beck, W. *J. Organomet. Chem.* **1987**, *319*, C1–C4.

(6) (a) Bell, S. A.; Lancaster, J. C.; McWhinnie, W. R. *Inorg. Nucl. Chem. Lett.* **1971**, *7*, 405–407. (b) Mayfield, H. G., Jr.; Bull, W. E. *J. Chem. Soc. A* **1971**, 2279–2281. (c) Regina, F. J.; Wojcicki, A. *Inorg. Chem.* **1980**, *19*, 3803–3807. (d) Bauer, H.; Nagel, U.; Beck, W. *J. Organomet. Chem.* **1985**, *290*, 219–229.

(7) (a) Mews, R. *Angew. Chem., Int. Ed. Engl.* **1975**, *14*, 640. (b) Sünkel, K.; Nagel, U.; Beck, W. *J. Organomet. Chem.* **1983**, *251*, 227–243.

(8) (a) Siedle, A. R.; Newmark, R. A.; Pignolet, L. H. *Inorg. Chem.* **1986**, *25*, 3412–3418. (b) Noirot, M. D.; Anderson, O. P.; Strauss, S. H. *Ibid.* **1987**, *26*, 2216–2223. (c) Gupta, G. P.; Lang, G.; Lee, Y. J.; Scheidt, W. R.; Shelly, K.; Reed, C. A. *Ibid.* **1987**, *26*, 3022–3030.

(9) (a) Schrenk, J. L.; Palazzotto, M. C.; Mann, K. R. *Inorg. Chem.* **1983**, *22*, 4047–4049. (b) Boyd, D. C.; Rodman, G. S.; Mann, K. R. *J. Am. Chem. Soc.* **1986**, *108*, 1779–1784.

(10) (a) Gillespie, R. J.; Peel, T. E. *Adv. Phys. Org. Chem.* **1971**, *9*, 1–24. (b) Liang, J. J.-N. Ph.D. Dissertation, McMaster University, Hamilton, Canada, 1977. (c) Devynck, J.; Hadid, A. B.; Fabre, P. L.; Trémillon, B. *Anal. Chim. Acta* **1978**, *100*, 343–352. (d) O'Donnell, T. A. *J. Fluorine Chem.* **1984**, *25*, 75–82. (e) Gillespie, R. J.; Liang, J. *J. Am. Chem. Soc.* **1988**, *110*, 6053–6057.

(11) (a) Olah, G. A.; Baker, E. B.; Evans, J. C.; Tolgyesi, W. S.; McIntyre, J. S.; Bastien, I. J. *J. Am. Chem. Soc.* **1964**, *86*, 1360–1373. (b) Olah, G. A.; Pittman, C. U., Jr. *Adv. Phys. Org. Chem.* **1966**, *4*, 305–347. (c) Bacon, J.; Dean, P. A. W.; Gillespie, R. J. *Can. J. Chem.* **1969**, *47*, 1655–1659. (d) Commeyras, A.; Olah, G. A. *J. Am. Chem. Soc.* **1969**, *91*, 2929–2942. (e) Olah, G. A.; White, A. M. *Ibid.* **1969**, *91*, 5801–5810. (f) Kirchen, R. P.; Sorensen, T. S. *Ibid.* **1977**, *99*, 6687–6693. (g) Olah, G. A.; Donovan, D. J. *Ibid.* **1978**, *100*, 5163–5169. (h) Arnett, E. M.; Petro, C. *Ibid.* **1978**, *100*, 5408–5416. (i) Finne, E. S.; Gunn, J. R.; Sorensen, T. S. *Ibid.* **1987**, *109*, 7816–7823.

(12) (a) Bacon, J.; Dean, P. A. W.; Gillespie, R. J. *Can. J. Chem.* **1970**, *48*, 3413–3424. (b) Bacon J.; Dean, P. A. W.; Gillespie, R. J. *Ibid.* **1971**, *49*, 1276–1283. (c) McRae, V. M.; Peacock, R. D.; Russell, D. R. *J. Chem. Soc., Chem. Commun.* **1969**, 62–63. (d) Lind, M. D.; Christe, K. O. *Inorg. Chem.* **1972**, *11*, 608–612. (e) McKee, D. E.; Zalkin, A.; Bartlett, N. *Ibid.* **1973**, *12*, 1713–1717. (f) Edwards, A. J.; Taylor, P. *J. Chem. Soc., Dalton Trans.* **1973**, 2150–2153. (g) Edwards, A. J.; Sills, R. J. C. *Ibid.* **1974**, 1726–1729. (h) Gillespie, R. J.; Riddell, F. G.; Slim, D. R. *J. Am. Chem. Soc.* **1976**, *98*, 8069–8072. (i) Clegg, W.; Glemser, O.; Harms, K.; Hartmann, G.; Mews, R.; Noltemeyer, M.; Sheldrick, G. M. *Acta Crystallogr., Sect. B* **1981**, *B37*, 548–552.

(13) (a) Calves, J.-Y.; Gillespie, R. J. *J. Am. Chem. Soc.* **1977**, *99*, 1788–1792. (b) Clark, H. C.; O'Brien, R. J. *Inorg. Chem.* **1963**, *2*, 1020–1022.

(14) (a) Bougon, R.; Fawcett, J.; Holloway, J. H.; Russell, D. R. *J. Chem. Soc., Dalton Trans.* **1979**, 1881–1885. (b) Fawcett, J.; Holloway, J. H.; Russell, D. R. *Ibid.* **1981**, 1212–1218. (c) Fawcett, J.; Holloway, J. H.; Laycock, D.; Russell, D. R. *Ibid.* **1982**, 1355–1360.

(15) Hersh, W. H. *J. Am. Chem. Soc.* **1985**, *107*, 4599–4601.

(16) (a) Shelly, K.; Bartczak, T.; Scheidt, W. R.; Reed, C. A. *Inorg. Chem.* **1985**, *24*, 4325–4330. (b) Dean, P. A. W. *Inorg. Chim. Acta* **1986**, *114*, L1–L3.

(17) Honeychuck, R. V.; Hersh, W. H. *J. Am. Chem. Soc.*, in press.

Scheme I

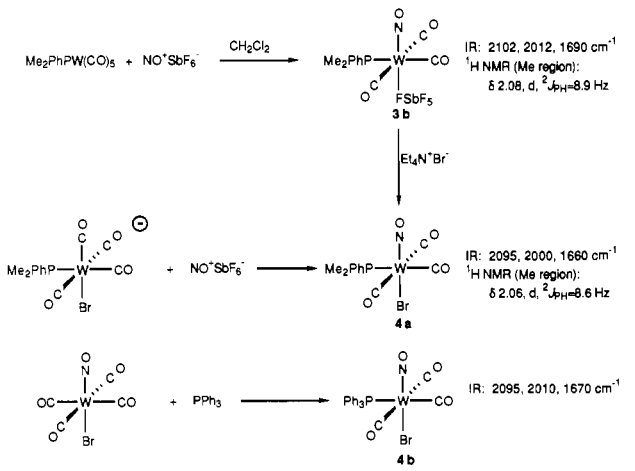

Scheme II

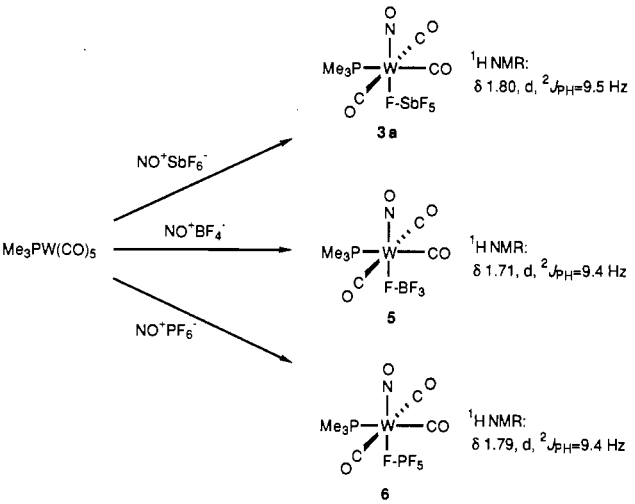

with formation of new bands near 2100 (m, sharp), 2010 (s), and 1690 (s) cm^{-1}. As shown in Scheme I for L = Me_2PhP, the addition of bromide ion resulted in a marked shift of the IR bands to lower frequency and in fact yielded a spectrum quite similar to that of known *mer*-$Ph_3PW(CO)_3(NO)Br$[18] (**4b**) as shown. With this in mind we nitrosylated [*cis*-$Me_2PhPW(CO)_4Br]^-$,[19] in a procedure analogous to that used to prepare *trans*-$W(CO)_4(NO)Br$.[20] Although the reaction was not clean, the IR as well as the ^1H NMR spectrum clearly included as the major bands those seen by bromide addition to **3b**. These infrared and synthetic results suggested that the initial nitrosylation product **3b** had the same overall geometry as **4b** and possessed a ligand trans to NO that was readily displaced by bromide ion. Initial evidence that the labile ligand was $[SbF_6]^-$ rather than the solvent CH_2Cl_2 was provided by ^1H NMR spectroscopy. Thus, nitrosylation of $Me_3PW(CO)_5$ with [NO][X] ($[X]^- = [SbF_6]^-$, $[BF_4]^-$, $[PF_6]^-$) each yielded a spectrum with a single doublet whose chemical shift and coupling constant were dependent on the nature of $[X]^-$ (Scheme II); the simplest explanation was that each of the "noncoordinating" anions $[SbF_6]^-$, $[BF_4]^-$, and $[PF_6]^-$ was coordinated to tungsten in **3a**, **5**, and **6**, respectively.

A certain amount of art was required to isolate the presumed adducts in *crystalline* form, even though on the basis of their infrared spectra the reactions were clean. For **3c** (L = Cy_3P), **5**, and **6**, the key to their isolation, albeit in low yield, lay in never stripping the nitrosylation reaction mixtures; the workup simply involved reducing the volume and/or adding hexanes, cooling, and

Scheme III

(as required) decanting the solution away from oily precipitates, followed by further concentration and crystallization from the resultant solution. The oily materials presumably contain minor (unidentified) impurities that hinder crystallization. In the case of $[SbF_6]^-$ adducts **3a,b**, larger scale and reproducibly high-yield procedures have been developed; here the key was the use of 1,1,2-trichlorotrifluoroethane as a solvent of polarity intermediate between that of hexane and methylene chloride to precipitate the unidentified impurities that presumably hinder crystallization. The isolated yellow crystalline compounds, while not obviously air-sensitive, are all quite hygroscopic and so are always handled under nitrogen. The $[SbF_6]^-$ adducts are reasonably thermally stable at room temperature, but storage for several months even at −40 °C gives rise to observable amounts of methylene chloride insoluble material. The $[BF_4]^-$ adduct **5** is qualitatively less stable thermally, while $[PF_6]^-$ adduct **6** does not survive even 2 days at room temperature. All but **6** gave acceptable C, H, and N elemental analyses, while **3a** was further successfully subject to P and F analysis. No elemental analysis of **6** was attempted; instead it was converted to acetonitrile adduct **7**, for which an acceptable

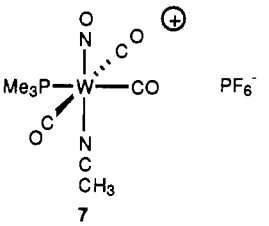

C, H, and N analysis was obtained. Lastly, mass spectra of **3a** and **3b** yielded no molecular ions, but WSb envelopes—tungsten has four abundant isotopes, antimony two[21]—corresponding to $[LW(CO)_2(NO)SbF_6]^+$ and $[LW(CO)(NO)SbF_6]^+$ (L = Me_3P, Me_2PhP) indicated that the tungsten and $[SbF_6]^-$ moieties were bound in the gas phase, and the observation of the $[LW(CO)_3NO]^+$ ions indicated that three carbonyl ligands were also bound to tungsten. It is also interesting to note that $[LW(CO)_n(NO)F]^+$ (n = 0, 1, 2) ions were also observed; this is the only evidence we have that cleavage of the W–F–SbF_5 linkage can occur at the F–Sb bond in addition to the F–W bond.

Substitution Reactions. Typical characterization of complexes of noncoordinating anions includes the demonstration that a variety of neutral ligands will readily displace the anion to give more tractable and characterizable cationic complexes.[3a,b,4h,n,5i,k,q,s,t,6c,7a,22] We have fully characterized the phosphine, nitrile, aldehyde, and ketone substitution adducts **8**–**12** shown in Scheme III, as well as **7** described above. An X-ray diffraction study of **11** showed the acrolein to be coordinated to tungsten in η^1-fashion via the carbonyl oxygen, and ^1H and ^{13}C NMR spectra provided evidence that this is the structure in solution as well.[23] We note however that we have been unable to obtain satisfactory elemental analyses on **11** and **12** and suspect the low carbon analyses are due to loss of the weakly bound volatile organic ligand from the solid com-

(18) Colton, R.; Commons, C. J. *Aust. J. Chem.* **1973**, *26*, 1487–1492.
(19) Schenk, W. A. *J. Organomet. Chem.* **1979**, *179*, 253–261.
(20) Barraclough, C. G.; Bowden, J. A.; Colton, R.; Commons, C. J. *Aust. J. Chem.* **1973**, *26*, 241–245.
(21) Gordon, A. J.; Ford, R. A. *The Chemist's Companion*; Wiley: New York, 1972.
(22) (a) Oltmanns, M.; Mews, R. *Z. Naturforsch., B* **1980**, *35B*, 1324–1325. (b) Urban, G.; Sünkel, K.; Beck, W. *J. Organomet. Chem.* **1985**, *290*, 329–339.
(23) (a) Honeychuck, R. V.; Bonnesen, P. V.; Farahi, J.; Hersh, W. H. *J. Org. Chem.* **1987**, *52*, 5293–5296. (b) Bonnesen, P. V.; Puckett, C. L.; Honeychuck, R. V.; Hersh, W. H. *J. Am. Chem. Soc.*, in press.

Table I. CO and NO Stretching Frequencies (cm^{-1}) in CH_2Cl_2 for Selected [*mer*-(*cis*-L)(*trans*-X)W(CO)$_3$NO]$^+$

L	X	ν(NO)[a]	ν(CO)		
			ν(A′)	ν(A′)	ν(A″)
Me_2PhP	Br^-	1660	2095	2000	2000
Me_3P	$[SbF_6]^-$	1690	2102	2010	2010
Me_3P	CH_3CN	1703	2102	2010	2010
Me_3P	Me_3P	1713	2080	2002	2002

[a] Vibrational mode A′.

pounds. In addition to the ligands in **8**–**12**, acetone, dimethyl sulfone, dimethylformamide, alcohols, water, tetrahydrofuran, triethylamine, P-donor ligands such as tricyclohexylphosphine and trimethyl phosphite, and the halides chloride, bromide, and iodide each immediately displaces $[SbF_6]^-$ from **3a** in CD_2Cl_2 solution, as judged by the loss of the characteristic phosphorus–fluorine coupling seen in the ^{31}P NMR spectrum (vide infra). It is interesting to note that a water complex[5i,j,t,6d,22a,24] was observed upon addition of 1 equiv of D_2O to $[SbF_6]^-$ adduct **3a**, but addition of 2 equiv of D_2O to $[PF_6]^-$ adduct **6** instead gave the $[PF_2O_2]^-$ adduct due to hydrolysis of the anion.[4h,6d,25] Coordination of the $[PF_2O_2]^-$ ion was clearly indicated by the 4.7-Hz coupling of the phosphorus atoms ($[PF_2O_2]^-$ to PMe_3), while oxygen rather than fluorine bonding to tungsten was indicated by the absence of any apparent fluorine–PMe_3 coupling in the ^{31}P NMR spectrum. Ligands that do *not* completely displace $[SbF_6]^-$ from **3a** upon addition of a single equivalent include diethyl ether, 2,2,2-trifluoroethanol, and carbon monoxide, while the S-donor ligand carbon disulfide does not diplace $[SbF_6]^-$ even when present at a concentration of 10% by volume in CD_2Cl_2. Carbon monoxide is a special case, in that displacement of $[SbF_6]^-$ is maintained only under a CO atmosphere; under a variety of conditions a mixture of what are apparently [*cis*- and *trans*-$(Me_3P)W(CO)_4(NO)][SbF_6]$ forms, the latter of which has been characterized crystallographically.[26] We have reported the results of a ^{31}P NMR study of these substitution adducts, in which a cis-influence series was observed on the basis of the correlation of $^1J(^{31}P–^{183}W)$ with $\delta(^{31}P)$ of the PMe_3 ligand for 20 substituents and in which the correlation of the cis-influence series with ligand donor strength was evident.[27]

Infrared Spectra. Cotton–Kraihanzel force constants[28] were calculated for each of the fully characterized compounds; full details of the calculations, input frequencies, and output force constants may be found in the supplementary material. The major conclusions from the calculations are that the proposed C_s point-group symmetry of these compounds is consistent with the observed IR spectra and that the frequencies and force constants are well correlated despite the coupling of three vibrations having the same symmetry; hence, the frequencies themselves can be referred to for discussion. There appears to be an increase in nitrosyl stretching frequency with increasing donor strength for the ligand (with the exception of Br^-) trans to NO, as seen for the representative examples in Table I. Literature treatments of infrared data do not predict such a trend—the trans ligand is expected to be sensitive to π rather than σ effects.[29] One explanation might be that the stronger the trans donor, the weaker the σ interaction of the nitrosyl ligand with the metal. This longer tungsten–nitrogen bond would weaken the π-back-bonding interaction and so raise ν(NO). Such an explanation is similar to that advanced to account for carbonyl stretching interactions in $Cr(CO)_6$.[29c] An alternative explanation for our results is that they are an artifact caused by the requisite use of polar methylene chloride as the solvent, rather than more appropriate less polar solvents.[29b] In any case, the overall trend is less precise than the correlation of ligand donor strength that we have observed by ^{31}P NMR spectroscopy,[27a] precluding the development of such a quantitative IR correlation.

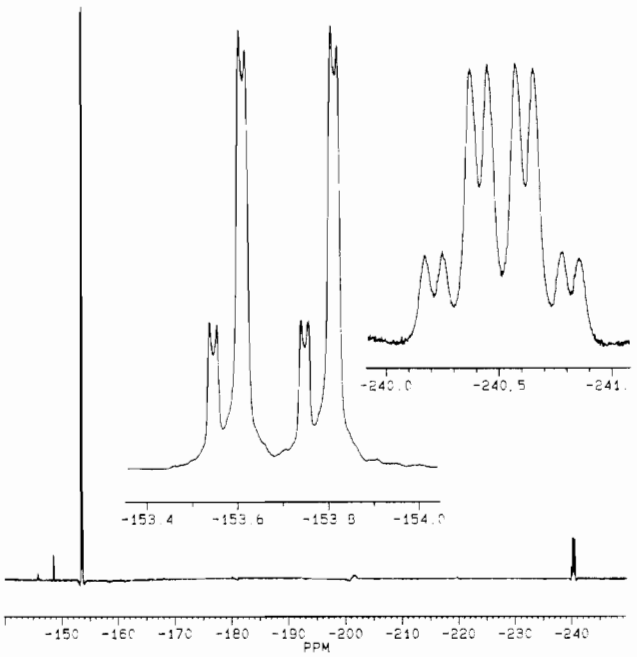

Figure 1. ^{19}F NMR spectrum of **5** (470.598 MHz; 185 K). The −240 ppm signal is plotted at half the expansion of the −153 ppm signals. The singlet at −148.7 ppm is due to free $[BF_4]^-$. The base-line ripples arise due to a 50-μs delay used prior to acquisition of the FID; this is the minimum delay that allows elimination of a broad signal (−180 ppm, $\nu_{1/2}$ ~15 000 Hz) due to fluorine in the NMR probe.

NMR Spectra. Definitive evidence for coordination of the noncoordinating anions in solution is provided by ^{19}F, ^{31}P, and ^{13}C NMR spectra, which exhibit *coupling* between the fluorine atoms on the anion and the phosphorus and carbon atoms attached to tungsten. The 471-MHz ^{19}F NMR spectrum of $[BF_4]^-$ adduct **5** additionally exhibits resolved signals due to bridging and terminal fluorine atoms (Figure 1). Thus, at 185 K, the spectrum consists of a small singlet assigned to free $[BF_4]^-$ at −148.7 ppm, a set of doublet of doublets at −153.65 ("J" = 7.3 Hz) and −153.71 ("J" = 6.2 Hz) ppm ($^2J_{FF}$ = 94.9 Hz) in a 1:4 ratio assigned to the three terminal fluorine atoms of the ^{10}B and ^{11}B isotopomers, and a broad doublet of quartets at −240.5 ppm ($^2J_{FF}$ = 95.4 ± 0.7 Hz, $^2J_{PF}$ = 36.3 ± 1.1 Hz) assigned to the bridging fluorine atom of the $[BF_4]^-$ ligand. In the latter upfield signal, the broadness is assumed to be due to overlapping signals due to the ^{10}B and ^{11}B isotopomers and to the quadrupole coupling to the ^{14}N nucleus of the trans-nitrosyl ligand—this latter effect was seen in the ^{31}P NMR spectra of **8** and **9** for the phosphorus atom trans to the nitrosyl ligand.[27a] We also assume that it is this broadening that results in the absence of any observed coupling to tungsten (14% of which is ^{183}W, $I = {}^1/_2$), due to either low intensity or J_{WF} < ~50 Hz. The cause of the 6–7 Hz doublet splitting of the signals due to the terminal fluorine atoms is not known; that it is *not* due to long-range phosphorus coupling is evident from the ^{31}P NMR spectrum, which does not exhibit such splitting (vide infra). One possible explanation is that the splitting is not due to coupling but rather is a chemical shift difference. While in principle this issue could be settled by acquiring data at a different field strength, in practice we have only once achieved sufficient resolution to observe this splitting at low temperature. We suggest that the

(24) Schloter, K.; Nagel, U.; Beck, W. *Chem. Ber.* **1980**, *113*, 3775–3782.
(25) Legzdins, P.; Oxley, J. C. *Inorg. Chem.* **1984**, *23*, 1053–1059.
(26) Honeychuck, R. V. Unpublished results. This work will be reported in detail separately.
(27) (a) Honeychuck, R. V.; Hersh, W. H. *Inorg. Chem.* **1987**, *26*, 1826–1828. (b) For a related trans-influence series, see: Olgemöller, B.; Beck, W. *Inorg. Chem.* **1983**, *22*, 997–998.
(28) (a) Cotton, F. A.; Kraihanzel, C. S. *J. Am. Chem. Soc.* **1962**, *84*, 4432–4438. (b) Cotton, F. A. *Chemical Applications of Group Theory*, 2nd ed.; Wiley-Interscience: New York, 1971; Chapter 10.
(29) (a) Graham, W. A. G. *Inorg. Chem.* **1968**, *7*, 315–321. (b) Brown, R. A.; Dobson, G. R. *Inorg. Chim. Acta* **1972**, *6*, 65–71. (c) Johnson, J. B.; Klemperer, W. G. *J. Am. Chem. Soc.* **1977**, *99*, 7132–7137. But for current quantitative views of σ and π bonding, see: (d) Bursten, B. E.; Freier, D. G.; Fenske, R. F. *Inorg. Chem.* **1980**, *19*, 1810–1811. (e) Ziegler, T.; Tschinke, V.; Ursenbach, C. *J. Am. Chem. Soc.* **1987**, *109*, 4825–4837.

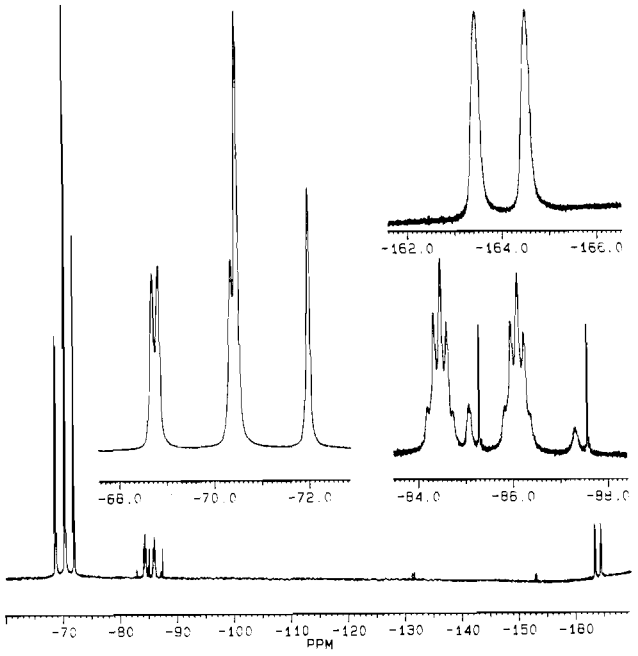

Figure 2. ^{19}F NMR spectrum of **6** (470.598 MHz; 185 K). The three expansions are plotted at the same scale. The sources of the minor doublets (see Experimental Section) are unknown; the sharp doublets are also visible at room temperature. The rise inthe base line above −160 ppm is due to the onset of a broad signal (−180 ppm, $\nu_{1/2}$ ~15000 Hz) due to fluorine in the NMR probe.

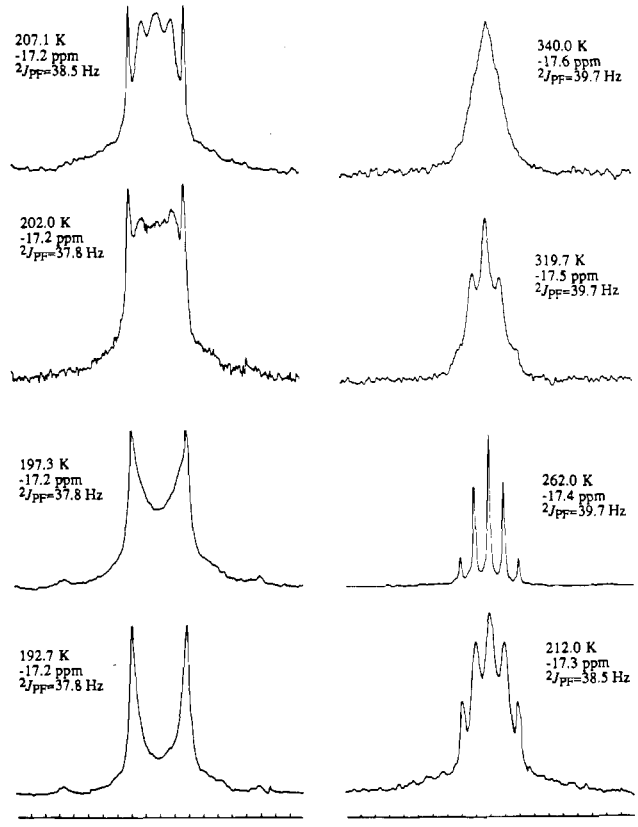

Figure 3. Variable-temperature ^{31}P NMR spectra of **5**. Scale markings are at 10-Hz intervals. The coupling constants are the true $^2J_{P(\mu\text{-}F)}$ values, not the peak separations. The small peaks within ±70 Hz of the center of the multiplets, most clearly visible at the two lowest temperatures, are spinning sidebands.

putative chemical shift differences are due to the presence of different conformers with respect to rotation of the BF_3 fragment about the W–F bond. Such an explanation would require a rotational barrier $\Delta G^{\ddagger} >$ ~10 kcal/mol, if one assumes that the rate is less than 10% of that at coalescence—that is, that the system is approaching the slow-exchange limit.[30] Warming the sample in the probe of the NMR spectrometer does not provide evidence for this hypothesis, however, since broadening of the signals due to exchange of the bridging and terminal resonances (vide infra) masks any broadening due to conformational exchange. We have also examined the ^{19}F NMR spectra of **3a** and **6**. Essentially no signal is observed for **3a**, presumably due to broadening due to efficient quadrupolar coupling[31] to the two antimony isotopes ($I = {}^5/_2, {}^7/_2$). For **6**, the room-temperature 339-MHz ^{19}F NMR spectrum exhibits a very broad doublet ($\nu_{1/2} \approx 550$ Hz for each line) at −88.3 ppm ($^1J_{PF} = 720$ Hz) along with a narrower but still broad doublet ($\nu_{1/2} = 85$ Hz) at −71.6 ppm ($^1J_{PF} = 708$ Hz), in a ~2:1 ratio. The major doublet is assigned to the η^1-$[PF_6]^-$ ligand of **6**, which is bound to tungsten but nevertheless exhibits rapid exchange of the bridging and terminal fluorine atoms via a process most readily described as anion "spinning" (vide infra). The minor doublet is near the position of free $[PF_6]^-$ (−73.5 ppm, $^1J_{PF} = 710$ Hz, for the $[(Ph_3P)_2N]^+$ salt in CD_2Cl_2), but the broadening of this signal suggests (as will be described below) that the $[PF_6]^-$ anion, rather than being free, may be weakly bound to an unidentified cation. The "spinning" process for the bound $[PF_6]^-$ ligand of **6** is frozen out at 471 MHz at 185 K, providing *the first example of coordinated* $[PF_6]^-$ *in which resolved signals for the bridging, equatorial, and axial fluorine atoms are seen*, in the expected 1:4:1 ratio (Figure 2). Thus, the equatorial fluorine atoms appear as a doublet of doublets at −69.6 ppm ($^1J_{PF} = 780$ Hz, $^2J_{FF} = 61 \pm 1$ Hz) that overlaps with the "free" $[PF_6]^-$ at −71.2 ppm ($^1J_{PF} = 710$ Hz), which is present in the same ratio as at room temperature, the axial fluorine appears as a doublet of quintets at −85.3 ppm ($^1J_{PF} = 764$ Hz, $^2J_{FF} = 63.6 \pm 1.9$ Hz), and the bridging fluorine atom appears as a broad doublet ($\nu_{1/2} \approx 92$ Hz for each peak) at −164.0 ppm ($^1J_{PF} = 497$ Hz). No coupling of the bridging fluorine atom to the terminal fluorine atoms is observed in the axial and equatorial resonances, and coupling to the PMe_3 ligand (vide infra) was not resolved, again presumably due to quadrupole coupling to the ^{14}N nucleus of the trans-nitrosyl ligand. Averaging of these low temperature signals would be expected to yield a doublet at −88.0 ppm ($^1J_{PF} = 730$ Hz) in the fast-exchange limit, in excellent agreement with the observed signal; the smaller observed coupling constant is expected, since even at the lower of the two magnetic fields used the sample is not yet at the fast-exchange limit.

The ^{31}P NMR spectrum at 193 K of $[BF_4]^-$ adduct **5** (Figure 3) exhibits a well-resolved doublet at −17.19 ppm ($^2J_{PF} = 37.84$ Hz); the coupling constant is the same within experimental error as that seen in the ^{19}F NMR spectrum, and the resolution is clearly sufficient to rule out any long-range coupling to the terminal fluorine atoms that would result in quartets with $^4J_{PF} = 6$–7 Hz were this the explanation of the doublet splitting of the low-field signals in the ^{19}F NMR spectrum. Upon warming of the sample in the probe of the NMR spectrometer, broadening of the doublet occurs followed by eventual sharpening at ~250 K to a well-resolved quintet. Without entering into any discussion of mechanism,[15,17] we propose that this process is due to anion "spinning", that is, a fluctional process that involves all four fluorine atoms exchanging into the bridging site, *but without the anion leaving the coordination sphere of the tungsten atom*. Upon further warming of the sample to ~340 K, the quintet coalesces to a broad singlet, the expected result of *intermolecular* anion exchange. The $[SbF_6]^-$ adduct **3a** exhibits qualitatively similar behavior (Figure 4), with a sharp doublet at 194 K at −15.43 ppm ($^2J_{PF} = 37.64$ Hz), a sharp *septet* at ~250–270 K, and a broad singlet at ~324 K. The $[PF_6]^-$ adduct **6** exhibits a faster rate of intramolecular exchange, so that even at 165 K only a broad doublet at −16.23 ppm ($^2J_{PF} = 39.5$ Hz) is observed; a sharp septet is observed at ~220 K, and this coalesces to a singlet by 306 K. Signals due to free and bound $[PF_6]^-$ were also observed in the ^{31}P NMR

(30) Leyden, D. E.; Cox, R. H. *Analytical Applications of NMR*; Wiley-Interscience: New York, 1977; pp 283–289.
(31) Bacon, J.; Gillespie, R. J. *J. Am. Chem. Soc.* **1971**, *93*, 6914–6919.

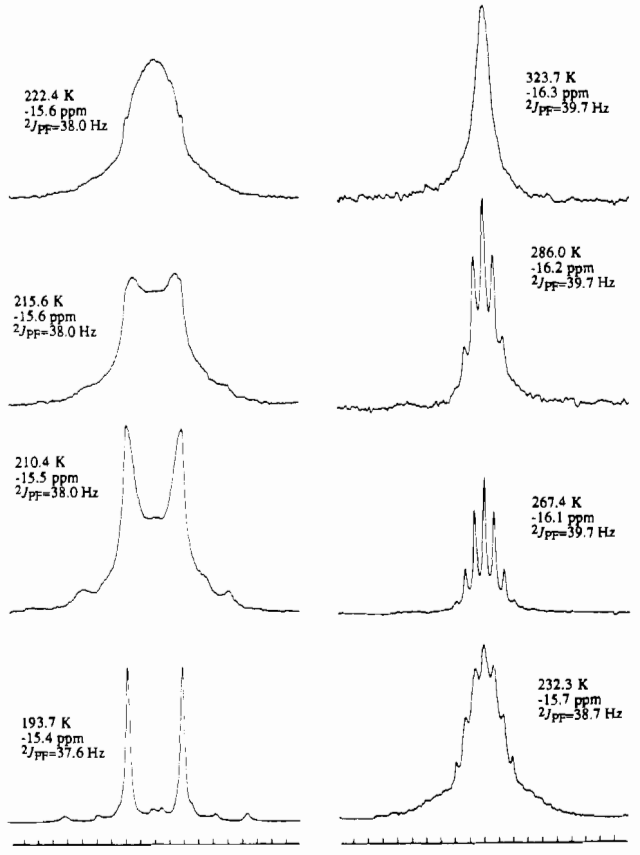

Figure 4. Variable-temperature ^{31}P NMR spectra of **3a**. Scale markings are at 10-Hz intervals. The coupling constants are the true $^2J_{P(\mu\text{-}F)}$ values, not the peak separations. The small peaks within ±70 Hz of the center of the multiplets, most clearly visible at the two lowest temperatures, are spinning sidebands.

spectra of **6**. At 165 K, the free anion appears as a sharp septet at −146.4 ppm ($^1J_{PF}$ = 712 Hz), while the bound $[PF_6]^-$ appears as a relatively sharp *sextet of doublets* at −142.7 ppm ($^1J_{P(\mu\text{-}F)}$ = 502 ± 3 Hz; $^1J_{PF(eq,ax)}$ = 776 ± 2 Hz,[17] where eq = equatorial, ax = axial, and av = average); we believe this to be the first example of ^{31}P NMR observation of bound $[PF_6]^-$ and obviously of differential P–F coupling due to coordination. The signals due to the bound $[PF_6]^-$ coalesce to a broad septet by 194 K, which sharpens at 221 K to a septet at −141.5 ppm ($^1J_{PF(av)}$ = 730.7 Hz). In all cases these PF coupling constants are in good agreement with those seen in the ^{19}F NMR spectrum at 185 K, where $^1J_{P(\mu\text{-}F)}$ = 497 Hz, the weighted average of the five terminal PF coupling constants is 777 ± 6 Hz, and $^1J_{PF(av)}$ = 730.2 Hz. While the signals due to bound $[PF_6]^-$ remain sharp to the highest temperature examined (306 K), those due to free $[PF_6]^-$ begin to broaden at 260 K and are scarcely visible at 306 K, although addition of excess $[(Ph_3P)_2N][PF_6]$ results in a readily observable, albeit broad, septet at −144 ppm. Addition of either CH_3CN or PMe_3 gives **7** or the $[PF_6]^-$ analogue of **8**, as well as a very sharp septet due to free $[PF_6]^-$ at −144.2 ppm ($^1J_{PF}$ = 710.2 Hz). These results suggest the presence of a ^{31}P NMR-silent impurity that interacts only with free $[PF_6]^-$ and like **6** also reacts with both PMe_3 and CH_3CN. One possibility is that a CD_2Cl_2 complex is present, since coordination of this solvent rather than $[PF_6]^-$ is known.[5i,j,l,32] However, the ratio of free to bound $[PF_6]^-$ is ~30:70, as was seen in the ^{19}F NMR spectrum, and no *singlet* peak corresponding to the PMe_3 fragment of such a species is visible. The major impurity observed in the ^{31}P NMR spectrum is a *doublet*, typically 10% of the intensity of the PMe_3 septet of **6**, at −17.35 ppm ($^2J_{PF}$ = 35.4 Hz). A reasonable possibility is that this is $Me_3P(CO)_3(NO)W\text{–}F$ (although no doublet having $^2J_{PF}$ = 35 Hz is seen in the ^{19}F NMR spectrum from −40 to −330 ppm),

(32) Fernández, J. M.; Gladysz, J. A. *Organometallics* **1989**, *8*, 207–219.

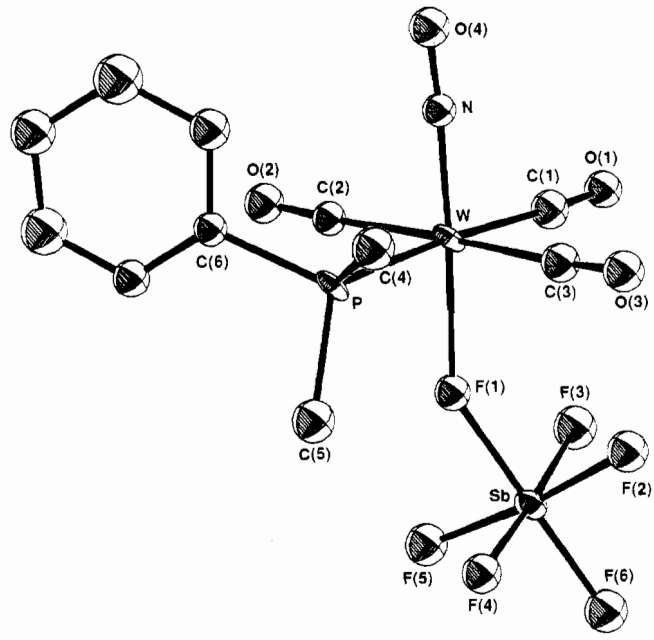

Figure 5. ORTEP drawing of **3b**.

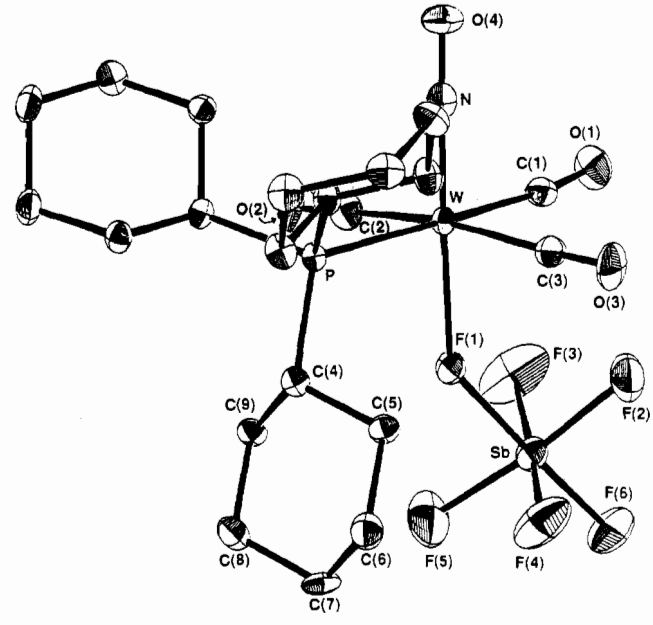

Figure 6. ORTEP drawing of **3c**.

a compound that we have been unable to generate in situ from **3a** and a variety of sources of F^-. Addition of CH_3CN results in the loss of this signal, which would be consistent with our conclusion that this fluoride adduct is unstable. In any case, at present the source of the free $[PF_6]^-$ remains unknown. Finally, it should be noted that, presumably due to the low stability of **6**, clean spectra are never obtained, but the above results—including the ratio of free to bound $[PF_6]^-$—are reproducible and are obtained both when X-ray quality crystals of **6** are used and when the nitrosylation of $Me_3PW(CO)_5$ with $[NO][PF_6]$ is carried out in situ in CD_2Cl_2.

The ^{13}C NMR spectra of **3a** and **5** also exhibit coupling to fluorine, although only that for **3a** was well resolved. Two doublet of septets are observed at 265 K for **3a**, at 201.41 ppm ($^2J_{CP}$ = 7.3 Hz, $^2J_{CF}$ = 11.1 ± 0.5 Hz) and at 201.45 ppm ($^2J_{CP}$ = 41.1 Hz, $^2J_{CF}$ = 9.8 ± 1.4 Hz), due, on the basis of intensity and $^2J_{CP}$,[33] to the carbonyls cis and trans to the PMe_3 ligand.

(33) (a) Todd, L. J.; Wilkinson, J. R. *J. Organomet. Chem.* **1974**, *77*, 1–25. (b) Bancroft, G. M.; Dignard-Bailey, L.; Puddephatt, R. J. *Inorg. Chem.* **1986**, *25*, 3675–3680.

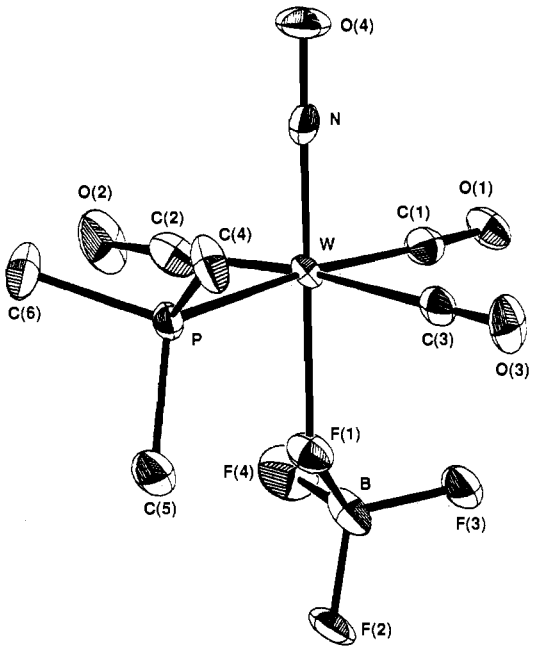

Figure 7. ORTEP drawing of **5**.

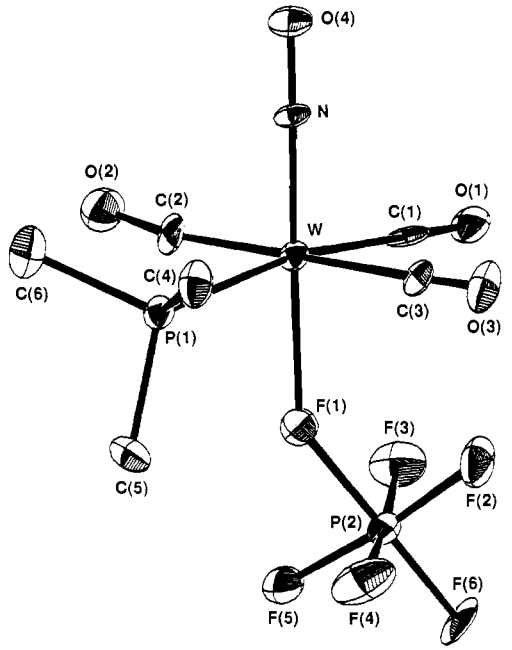

Figure 8. ORTEP drawing of **6**.

X-ray Diffraction Studies. Coordination of the anions $[SbF_6]^-$, $[BF_4]^-$, and $[PF_6]^-$ via a μ-F bridge to tungsten was confirmed through single-crystal X-ray structures of **3b**, **3c**, **5**, and **6** (Figures 5–8; selected bond distances and angles, Table II–V). The major experimental point to be addressed in the solution of these structures lies in the identification of the nitrosyl ligand. Initial identification of the nitrogen atom was made on the basis of the W–N bond lengths; for the four structures described in this work, the W–N bond lengths average 1.790 (3) Å, while the W–C bond lengths average 2.07 (2) Å. Differential N–O and C–O bond lengths are also seen, averaging 1.196 (15) and 1.13 (2) Å, respectively. These sets of values are typical of tungsten and molybdenum compounds.[34] Differences in the isotropic temperature factors are more definitive (Table VI). The isotropic temperature factors for carbon and nitrogen are relatively similar (as is reasonable), with that for the nitrogen atoms ranging from 64–98% of the average of that of the carbonyl carbon atoms. If the nitrogen atom is then labeled as a carbon atom and the refinement procedure is repeated,[35] virtually identical residuals (R and R_w) are obtained, but the isotropic temperature factors of these new "carbon" atoms are now unreasonably small, ranging from 8–48% of the average of that of the carbon atoms, with the decrease in

(34) See for instance: (a) Love, R. A.; Chin, H. B.; Koetzle, T. F.; Kirtley, S. W.; Whittlesey, B. R.; Bau, R. *J. Am. Chem. Soc.* **1976**, *98*, 4491–4498. (b) Bonnesen, P. V.; Baker, A. T.; Hersh, W. H. *Ibid.* **1986**, *108*, 8304–8305. (c) Holl, M. M.; Hillhouse, G. L.; Folting, K.; Huffman, J. C. *Organometallics* **1987**, *6*, 1522–1527. (d) Bonnesen, P. V.; Yau, P. K. L.; Hersh, W. H. *Ibid.* **1987**, *6*, 1587–1590.

(35) Gladfelter, W. L. *Adv. Organomet. Chem.* **1985**, *24*, 41–86.

Table II. Selected Distances (Å) and Angles (deg) in **3b**

W–F(1)	2.169 (11)	P–W–C(1)	175.36 (61)
W–P	2.518 (5)	P–W–C(2)	88.69 (57)
W–N	1.795 (17)	P–W–C(3)	88.09 (61)
W–C(1)	2.092 (23)	P–W–N	92.43 (52)
W–C(2)	2.089 (20)	C(2)–W–C(3)	176.49 (82)
W–C(3)	2.052 (21)	W–C(1)–O(1)	176.3 (19)
C(1)–O(1)	1.116 (24)	W–C(2)–O(2)	174.6 (18)
C(2)–O(2)	1.106 (22)	W–C(3)–O(3)	176.0 (19)
C(3)–O(3)	1.167 (24)	W–N–O(4)	177.9 (15)
N–O(4)	1.172 (20)	W–F(1)–Sb	147.15 (59)
Sb–F(1)	1.954 (11)	F(1)–Sb–F(2)	85.39 (48)
Sb–F(2)	1.878 (12)	F(1)–Sb–F(3)	87.53 (50)
Sb–F(3)	1.862 (12)	F(1)–Sb–F(4)	88.31 (48)
Sb–F(4)	1.855 (12)	F(1)–Sb–F(5)	88.10 (50)
Sb–F(5)	1.861 (12)	F(1)–Sb–F(6)	179.30 (48)
Sb–F(6)	1.864 (12)	F(2)–Sb–F(5)	173.46 (52)
F(1)–W–N	176.51 (57)	F(3)–Sb–F(4)	175.82 (53)
F(1)–W–P	86.43 (32)	F(6)–Sb–F(2)	93.91 (53)
F(1)–W–C(1)	89.47 (68)	F(6)–Sb–F(3)	92.35 (53)
F(1)–W–C(2)	89.32 (62)	F(6)–Sb–F(4)	91.79 (52)
F(1)–W–C(3)	89.08 (67)	F(6)–Sb–F(5)	92.59 (53)

Table III. Selected Distances (Å) and Angles (deg) in **3c**

W–F(1)	2.186 (3)	P–W–C(1)	176.96 (15)
W–P	2.588 (1)	P–W–C(2)	89.40 (15)
W–N	1.788 (5)	P–W–C(3)	94.49 (14)
W–C(1)	2.058 (5)	P–W–N	91.47 (14)
W–C(2)	2.078 (6)	C(2)–W–C(3)	170.23 (20)
W–C(3)	2.095 (6)	W–C(1)–O(1)	173.83 (51)
C(1)–O(1)	1.132 (6)	W–C(2)–O(2)	176.18 (46)
C(2)–O(2)	1.128 (7)	W–C(3)–O(3)	176.09 (47)
C(3)–O(3)	1.126 (7)	W–N–O(4)	178.71 (39)
N–O(4)	1.210 (6)	W–F(1)–Sb	138.90 (15)
Sb–F(1)	1.979 (3)	F(1)–Sb–F(2)	85.20 (14)
Sb–F(2)	1.868 (4)	F(1)–Sb–F(3)	85.05 (16)
Sb–F(3)	1.855 (4)	F(1)–Sb–F(4)	87.70 (16)
Sb–F(4)	1.858 (4)	F(1)–Sb–F(5)	87.28 (15)
Sb–F(5)	1.832 (4)	F(1)–Sb–F(6)	177.43 (16)
Sb–F(6)	1.857 (3)	F(2)–Sb–F(5)	172.48 (17)
F(1)–W–N	178.43 (14)	F(3)–Sb–F(4)	172.65 (19)
F(1)–W–P	89.87 (8)	F(6)–Sb–F(2)	93.13 (17)
F(1)–W–C(1)	90.16 (17)	F(6)–Sb–F(3)	92.99 (19)
F(1)–W–C(2)	85.22 (18)	F(6)–Sb–F(4)	94.23 (19)
F(1)–W–C(3)	85.82 (17)	F(6)–Sb–F(5)	94.39 (18)

Table IV. Selected Distances (Å) and Angles (deg) in **5**

W–F(1)	2.168 (7)	F(1)–W–C(3)	85.63 (39)
W–P	2.516 (3)	P–W–C(1)	174.98 (34)
W–N	1.788 (11)	P–W–C(2)	89.95 (37)
W–C(1)	2.075 (13)	P–W–C(3)	88.82 (31)
W–C(2)	2.091 (15)	P–W–N	93.04 (35)
W–C(3)	2.091 (13)	C(2)–W–C(3)	174.20 (48)
C(1)–O(1)	1.121 (14)	W–C(1)–O(1)	177.6 (10)
C(2)–O(2)	1.125 (16)	W–C(2)–O(2)	177.7 (12)
C(3)–O(3)	1.118 (15)	W–C(3)–O(3)	179.4 (11)
N–O(4)	1.208 (13)	W–N–O(4)	179.67 (94)
B–F(1)	1.500 (14)	W–F(1)–B	128.12 (72)
B–F(2)	1.386 (16)	F(1)–B–F(2)	104.08 (98)
B–F(3)	1.373 (16)	F(1)–B–F(3)	105.3 (10)
B–F(4)	1.316 (18)	F(1)–B–F(4)	107.8 (11)
F(1)–W–N	178.24 (39)	F(2)–B–F(3)	111.0 (12)
F(1)–W–P	85.65 (20)	F(2)–B–F(4)	113.7 (11)
F(1)–W–C(1)	89.48 (37)	F(3)–B–F(4)	114.1 (12)
F(1)–W–C(2)	88.62 (43)		

Table V. Selected Distances (Å) and Angles (deg) in **6**

W–F(1)	2.187 (10)	P(1)–W–C(1)	170.62 (44)
W–P(1)	2.534 (5)	P(1)–W–C(2)	87.86 (52)
W–N	1.789 (13)	P(1)–W–C(3)	91.85 (54)
W–C(1)	2.072 (17)	P(1)–W–N	97.22 (44)
W–C(2)	2.040 (19)	C(2)–W–C(3)	179.67 (66)
W–C(3)	2.061 (20)	W–C(1)–O(1)	177.3 (16)
C(1)–O(1)	1.116 (20)	W–C(2)–O(2)	172.5 (16)
C(2)–O(2)	1.174 (22)	W–C(3)–O(3)	177.3 (15)
C(3)–O(3)	1.124 (21)	W–N–O(4)	178.1 (13)
N–O(4)	1.192 (17)	W–F(1)–P(2)	142.35 (59)
P(2)–F(1)	1.733 (11)	F(1)–P(2)–F(2)	87.45 (56)
P(2)–F(3)	1.585 (13)	F(1)–P(2)–F(3)	87.12 (60)
P(2)–F(4)	1.550 (13)	F(1)–P(2)–F(4)	86.90 (63)
P(2)–F(2)	1.574 (12)	F(1)–P(2)–F(5)	86.83 (58)
P(2)–F(5)	1.569 (11)	F(1)–P(2)–F(6)	179.25 (60)
P(2)–F(6)	1.567 (10)	F(3)–P(2)–F(4)	173.99 (69)
F(1)–W–N	179.08 (50)	F(2)–P(2)–F(5)	174.19 (69)
F(1)–W–P(1)	83.49 (30)	F(6)–P(2)–F(2)	93.16 (63)
F(1)–W–C(1)	87.14 (52)	F(6)–P(2)–F(3)	92.44 (68)
F(1)–W–C(2)	91.06 (56)	F(6)–P(2)–F(4)	93.54 (68)
F(1)–W–C(3)	89.06 (55)	F(6)–P(2)–F(5)	92.56 (65)

temperature factor ranging from 51–88%. These data strongly support the proposed atomic identities.

Discussion

Synthesis. The synthesis of tungsten nitrosyl compounds using $[NO]^+$ salts is well known, and as shown for **13** and **14** in Scheme IV, substitution of a single CO ligand can occur. The reaction with **13** is deceptively simple: when carried out in methylene chloride, the reaction proceeds in good yield,[20] but we and others have been unable to separate the nitrosyl halide product from the $W(CO)_6$ byproduct.[36] The product can be obtained pure, albeit only in about 20% yield, if the reaction is carried out in acetonitrile, since the $W(CO)_6$ is then converted to dinitrosyl dications.[36c] We have found that $W(CO)_6$ reacts only very slowly in methylene chloride, the reaction likely proceeding in a manner analogous to that of $Mo(CO)_6$ as shown, which gives polymeric $Mo(NO)_2(PF_6)_2$;[25] this substitution of the noncoordinating anion $[PF_6]^-$ for CO is of course analogous to the reactions described here (Scheme II). On the basis of infrared data, we have found that $Ph_3PW(CO)_5$ reacts similarly to $W(CO)_6$, in that only dinitrosyl dications form, but as described above, replacement of even a single phenyl group of the Ph_3P ligand with an alkyl group allows formation of the mononitrosyl/$[SbF_6]^-$ adducts. We suggest that a ligand of stronger σ-donor ability than CO or PPh_3,[27a] and/or weaker π-acceptor ability, is required for the reaction to stop at the mononitrosyl stage. Further suggestive evidence in support of this hypothesis is our observation that $CH_3CNW(CO)_5$ yields mononitrosyl cations[37] and the reaction of **14** in Scheme IV, in which substitution of the second CO ligand is sufficient to tip the balance in favor of monosubstitution.[4n,38] These latter reactions as well as the synthesis of **3a** represent the highest yield syntheses of pure mononitrosyl tungsten carbonyl compounds.

The most straightforward mechanistic pathway to **3a** is that shown in Scheme V, in which simple CO substitution cis to the non-carbonyl ligand, as might be expected,[39] occurs to give **15**. The rapidity of this reaction (as well as all such nitrosylations) suggests that this is not a simple displacement reaction. In general, $LW(CO)_5$ compounds (and certainly for L = PR_3) undergo relatively slow CO dissociation, and rapid bimolecular (associative) substitution reactions are similarly unknown;[39a,b] to the extent that

Scheme IV

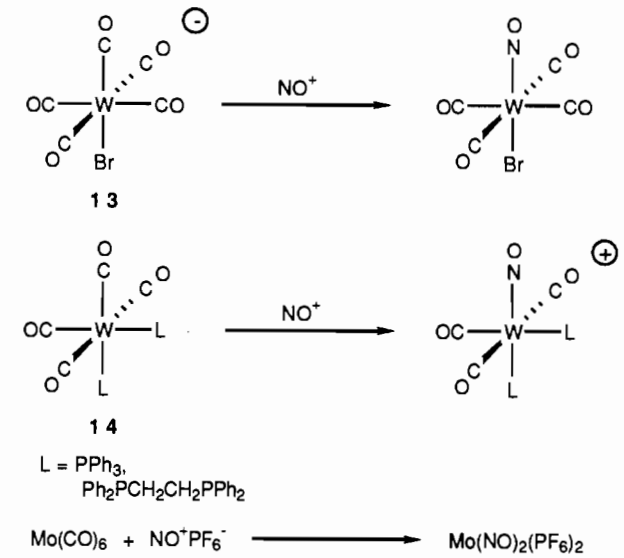

Scheme V

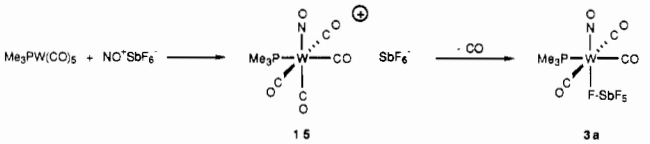

NO^+ is isoelectronic with CO, it would be expected to be a weak nucleophile. Some type of electron-transfer pathway is more likely,[40] although detailed speculation is not warranted at present. Regardless of the details of the formation of **15**, once formed, it would be expected to be unstable in solution with respect to loss of the CO trans to NO; only one other example of this arrangement of ligands is known for octahedral compounds, namely $V(CO)_5(NO)$, and it loses the trans CO rapidly below room temperature.[41] In the case of **15**, loss of CO from the reaction mixture allows coordination of the only available ligand, namely the noncoordinating anions $[SbF_6]^-$, $[BF_4]^-$, or $[PF_6]^-$. Regeneration of **15** from **3a** under modest pressures of carbon monoxide suggests that CO is in fact a better ligand than $[SbF_6]^-$ but is dissociatively (and obviously irreversibly) lost under the reaction conditions.[26]

Solution-State Structure. The low-temperature NMR data provide definitive evidence of coordination of $[SbF_6]^-$, $[BF_4]^-$, and $[PF_6]^-$ in solution. The ^{19}F NMR spectrum of $[BF_4]^-$ adduct **5** shows that the symmetry of the tetrahedral anion has been broken, on the basis of resonances assigned to terminal and bridging fluorine atoms that are separated by 87 ppm, and that coupling of the bridging fluorine to another nucleus is present. That this is the phosphorus atom bound to tungsten is shown by the ^{31}P NMR spectrum, which exhibits a doublet with the same J_{PF} seen in the ^{19}F NMR spectrum. These results demonstrate ligation of $[BF_4]^-$ via a single μ-F ligand and that it is in the coordination sphere of the tungsten. The ^{31}P NMR spectra of the $[SbF_6]^-$ and $[PF_6]^-$ adducts **3a–c** and **6** likewise demonstrate coordination of these anions. The dynamic behavior of these materials upon warming in the NMR probe, which we describe as an *intra*mo-

(36) (a) King, R. B.; Saran, M. S.; Anand, S. P. *Inorg. Chem.* **1974**, *13*, 3038–3040. (b) Legzdins, P.; Malito, J. T. *Ibid.* **1975**, *14*, 1875–1878. (c) Isaacs, E. E.; Graham, W. A. G. *J. Organomet. Chem.* **1975**, *99*, 119–126.

(37) Hersh, W. H. Manuscript in preparation.

(38) (a) Connelly, N. G. *J. Chem. Soc., Dalton Trans.* **1973**, 2183–2188. (b) Connor, J. A.; Riley, P. I.; Rix, C. J. *Ibid.* **1977**, 1317–1323.

(39) (a) Angelici, R. J. *Organomet. Chem. Rev.* **1968**, *3*, 173–226. (b) Dobson, G. R. *Acc. Chem. Res.* **1976**, *9*, 300–306. (c) Atwood, J. D.; Brown, T. L. *J. Am. Chem. Soc.* **1976**, *98*, 3160–3166. (d) Lichtenberger, D. L.; Brown, T. L. *Ibid.* **1978**, *100*, 366–373.

(40) See for instance: (a) Hershberger, J. W.; Klingler, R. J.; Kochi, J. K. *J. Am. Chem. Soc.* **1982**, *104*, 3034–3043. (b) Hershberger, J. W.; Klingler, R. J.; Kochi, J. K. *Ibid.* **1983**, *105*, 61–73. (c) Philbin, C. E.; Granatir, C. A.; Tyler, D. R. *Inorg. Chem.* **1986**, *25*, 4806–4807. (d) Kowaleski, R. M.; Basolo, F.; Trogler, W. C.; Gedridge, R. W.; Newbound, T. D.; Ernst, R. D. *J. Am. Chem. Soc.* **1987**, *109*, 4860–4869. (e) Dixon, A. J.; Gravelle, S. J.; van de Burgt, L. J.; Poliakoff, M.; Turner, J. J.; Weitz, E. *J. Chem. Soc. Chem. Commun.* **1987**, 1023–1025.

(41) Fjare, K. L.; Ellis, J. E. *J. Am. Chem. Soc.* **1983**, *105*, 2303–2307. The only other related compound of which we are aware is a *thio*nitrosyl compound, $[Re(CO)_5(NS)]^{2+}$: Mews, R.; Liu, C.-S. *Angew. Chem., Int. Ed. Engl.* **1983**, *22*, 162.

Table VI. Effect of Atom Identity on Isotropic Temperature Factor (B) of Nitrosyl Nitrogen

		nitrogen labeled as N		nitrogen labeled as C		
compd	B(C)[a]	B(N)[b]	% B(N)/B(C)	B("C")[c]	% B("C")/B(C)	% decrease[d]
$Me_2PhP(CO)_3(NO)W(\mu\text{-}F)SbF_5$ (**3b**)	2.13	1.68	79%	0.41	19%	76
$Cy_3P(CO)_3(NO)W(\mu\text{-}F)SbF_5$ (**3c**)	1.96	1.59	81%	0.65	33%	59
$Me_3P(CO)_3(NO)W(\mu\text{-}F)BF_3$ (**5**)	2.11	2.06	98%	1.01	48%	51
$Me_3P(CO)_3(NO)W(\mu\text{-}F)PF_5$ (**6**)	1.76	1.13	64%	0.14	8%	88

[a] Average of equivalent isotropic temperature factors (B's, in Å^2) of carbonyl carbons. [b] Equivalent isotropic temperature factor (B) of nitrosyl nitrogen. [c] Isotropic temperature factor in final refinement cycle for a *carbon* atom at position of nitrosyl *nitrogen* atom. [d] $[B(N) - B("C")]/B(N)$.

lecular spinning process followed at higher temperatures by an *inter*molecular exchange, is dependent on solvent, phosphine ligand, and the anion; the detailed description of these data and their mechanistic interpretation will be presented elsewhere.[17]

A few comparisons to literature ^{31}P, ^{19}F, and ^{13}C NMR data are available. We first compare ^{31}P NMR data in which coupling to fluorine–that is, $^2J_{PF}$—has been observed. Fischer reported that compound **16**, in which the isoelectronic carbyne ligand is sub-

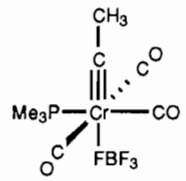

16

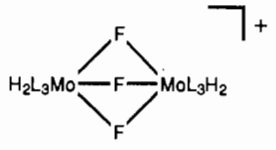

17 (L = $MePh_2P$)

stituted for the NO ligand of **5**, exhibited a quintet in the ^{31}P NMR spectrum at −20 °C.[5o] This result obviously now can be interpreted in terms of anion spinning, and the reported data yields J_{PF} = 35.2 Hz, compared to 39.7 Hz in **5**. Beck has reported ^{31}P NMR spectra for $Cp(CO)_2(PR_3)M(\mu\text{-}F)BF_3$ (R = Ph, OPh; M = Mo, W) and has observed doublets ($^2J_{PF}$ = 8–58 Hz) below −40 °C that give rise to quintets due to anion spinning upon warming to 10 °C.[5j] The large variation in $^2J_{PF}$ may be due to the nonoctahedral geometry, as well as the presence of cis and trans isomers. The sterically unhindered tungsten nitrosyl adducts **3a**, **3b**, **5**, and **6** exhibit $^2J_{PF}$ = 40 ± 2 Hz and hence no indication of relative donor strengths of the anions; the presumably more hindered Cy_3P adduct **3c** has $^2J_{PF}$ = 27 Hz. The values of these coupling constants may be compared to those involving a *terminal* fluorine ligand in isoelectronic octahedral tungsten and molybdenum compounds, where $^2J_{PF}$ = 30–43 Hz, and to that involving a *bridging* fluorine ligand in molybdenum compound **17**, where $^2J_{PF}$ = 35 Hz.[4n,42] The similarity in the magnitudes of these coupling constants suggests either that $^2J_{PF}$ is not sensitive to the degree of fluorine–phosphorus interaction or that the degree of bonding in these adducts of noncoordinating anions is in fact quite substantial.

A few $[BF_4]^-$ adducts exhibit ^{19}F NMR signals—in some cases broad—near the position of the *free* anion,[4k,5h,l] but others exhibit a broad singlet significantly upfield of the free anion, consistent with the *bound* anion spinning in the fast-exchange limit.[5p,w] Beck was the first to observe separate signals for the terminal and bridging fluorine atoms in $[BF_4]^-$ adducts, in the ^{19}F NMR spectra of $Cp(CO)_{3-n}(PR_3)_nM(\mu\text{-}F)BF_3$ (R = Ph, OPh, Me, Et; n = 0, 1; M = Mo, W).[5j,x] The terminal fluorine atoms were observed as a doublet near −156 ppm at temperatures below −51 °C, and the bridging fluorine atom was observed as a quartet or doublet of quartets (for the phosphine adducts) at −354 to −418 ppm, with $^2J_{FF}$ = 90–99 Hz and $^2J_{PF}$ = 19–58 Hz; the spectrum of $[BF_4]^-$ adduct **5**, having the terminal fluorine resonances near −154 ppm and the μ-F at −240.5 ppm ($^2J_{FF}$ = 95 Hz, $^2J_{PF}$ = 36 Hz), is thus quite similar. The only other results that are comparable were reported by Dean, who described ^{19}F NMR spectra of $[(en)_2Co\{(\mu\text{-}F)EF_5\}_2][EF_6]$ (en = 1,2-diaminoethane, E = Sb, As);[16b] for the antimony compound, for instance, signals of the expected splitting patterns were observed at −308.3, −111.4, and −131.8 ppm for the bridging, equatorial, and axial fluorine atoms, respectively, with $^2J_{FF}$ = 77 and 104 Hz for the bridging–equatorial and equatorial–axial pairs, respectively. Observation of such fluorine resonances and coupling has been known for some time, as noted in the introduction for **1**[11c,d,12a,b] and $CH_3\text{–}F\text{–}SbF_5$,[11g,13a] but the enormous upfield shifts for the bridging fluorine atoms are seen only upon coordination of the main-group fluoro anion to a transition metal.[43]

Both ^{19}F and ^{31}P NMR have been used to examine $[PF_6]^-$ adducts, and in all but one case only signals near the position of the free anion were seen.[4k,5l,6c,d] The one report of NMR evidence for $[PF_6]^-$ coordination is Beck's observation of a broad doublet (−111.3 ppm, $^1J_{PF}$ = 710 Hz) at −10 °C in the ^{19}F NMR spectrum of $Cp(CO)_3Mo(\mu\text{-}F)PF_5$; below −20 °C only a signal due to free $[PF_6]^-$ (−70.5 ppm, $^1J_{PF}$ = 714 Hz) was observed, leading to the suggestion that coordination of CH_2Cl_2[5l,32] is favored at low temperature and $[PF_6]^-$ at high temperature.[5j] Our ^{19}F NMR spectrum for **6** similarly exhibits a broad doublet at room temperature (−88.3 ppm, $^1J_{PF}$ = 720 Hz) due to bound $[PF_6]^-$, but disappearance of this signal by cooling (by 243 K) is due not to coordination of CD_2Cl_2 but to coalescence of the bridging and terminal fluorine resonances—upon further cooling, the observed bound:free $[PF_6]^-$ ratio of ~2:1 is unchanged. Only at the lowest temperature (185 K) and the highest field (471 MHz) available to us have we been able to obtain the first example of coordinated $[PF_6]^-$ in the slow-exchange (that is, nonspinning) limit. The chemical shifts and coupling constants of the terminal fluorine atoms are unexceptional, being similar to those of free $[PF_6]^-$, while the bridging fluorine atom like that in $[BF_4]^-$ adduct **5** is about 90 ppm to higher field. Our ^{31}P NMR data for **6** clearly show that $[PF_6]^-$ is bound at 165–306 K, on the basis of both the PMe_3 and $[PF_6]^-$ regions of the spectrum. The phosph*ine* signal exhibits coupling to the $[PF_6]^-$ fluorine atoms, while in the phosph*ate* region the bound anion is shifted 4 ppm downfield from the free anion; the free and bound anions do *not* exchange. In both regions of the spectrum, the chemical shifts are essentially unchanged over the temperature range examined, as is the ratio of bound:free anion, showing that **6** is not in equilibrium with another compound and that the changes that occur are due only to intra- and intermolecular anion exchange. In particular, the absence of any chemical shift changes under conditions of *inter*molecular $[PF_6]^-$ exchange in **6** is consistent with Beck's suggestion that anion coordination is preferred over CH_2Cl_2 coordination at high temperature. Our observation of a sharp signal for free $[PF_6]^-$ at low temperature that broadens at high temperature would also be consistent with Beck's suggestion, if an NMR-silent impurity binds CH_2Cl_2 at low temperature but then begins to bind free $[PF_6]^-$ as the temperature is raised. Finally, two phosphorus–fluorine coupling constants are observed in the low-temperature ^{31}P NMR spectrum of **6**, due to the presence of nonexchanging bridging and terminal fluorine atoms. While no precedent for this observation exists, a ^{19}F NMR spectrum of $[F_5P(\mu\text{-}F)SbF_5]^-$ has been reported,[44] and the terminal fluorine atoms have been attributed to signals having $^1J_{PF}$ = 913 or 940 Hz. The assignment is uncertain, and on the basis of our results, it is open to question, but it is made by comparison to PF_5 ($^1J_{PF}$

(42) (a) Hidai, M.; Mizobe, Y.; Sato, M.; Kodama, T.; Uchida, Y. *J. Am. Chem. Soc.* **1978**, *100*, 5740–5748. (b) Connor, J. A.; James, E. J.; Overton, C.; Walshe, J. M. A.; Head, R. A. *J. Chem. Soc., Dalton Trans.* **1986**, 511–515. (c) Crabtree, R. H.; Hlatky, G. G.; Holt, E. M. *J. Am. Chem. Soc.* **1983**, *105*, 7302–7306.

(43) Brownstein, S. *Inorg. Chem.* **1973**, *12*, 584–589.
(44) Brownstein, S. *Can. J. Chem.* **1969**, *47*, 605–609.

= 947 Hz) and to $[PF_6]^-$ ($^1J_{PF}$ = 711 Hz). The coupling constants in **6** of $^1J_{PF(t)} \approx 780$ and $^1J_{P(\mu\text{-}F)} \approx 500$ Hz (t = terminal) therefore suggest that while the $[PF_6]^-$ fragment is perturbed upon binding, it cannot be thought of as PF_5 loosely bound to $Me_3P(CO)_3(NO)W\text{-}F$.

The final NMR comparison that may be made is to the ^{13}C NMR spectra of carbyne **16** and related carbynes.[50,p] Only the carbyne carbon, located trans to the $[BF_4]^-$ ligand, exhibited any coupling to fluorine, as evidenced by the observation of a broad singlet or multiplet. Carbon–fluorine coupling was evident in $[BF_4]^-$ adduct **5**, but it was not well resolved, while the septets ($^2J_{CF}$ = 10–11 Hz) due to anion spinning in $[SbF_6]^-$ adduct **3a** were resolved with difficulty due to the line spacings of <2 Hz. We suspect it is for this reason in general that C–F coupling has not been observed previously in the ^{13}C NMR spectra, and this is clearly not the method of choice for demonstrating coordination of these anions.

Solid-State Structure: Length of the W–F Bond. The most striking feature of the solid-state structures of **3b**, **3c**, **5**, and **6** is the coordination of the noncoordinating anions via the fluorine bridge, and the most obvious question concerns the relative length of the W–F bond. While we have qualitatively observed that the order of stability of the anion complexes is $[SbF_6]^- > [BF_4]^- > [PF_6]^-$, the X-ray data reveal only small differences, albeit generally in the expected directions. Thus, $Me_2PhP/[SbF_6]^-$ complex **3b** and $[BF_4]^-$ complex **5** have the shortest W–F bonds (2.17 (1) Å) and the unstable $[PF_6]^-$ complex **6** has the longest W–F bond (2.19 (1) Å), while the sterically hindered $Cy_3P/[SbF_6]^-$ complex **3c** has a similarly long W–F bond (2.186 (3) Å). We first compare these numbers with those of other tungsten compounds that possess bridging and/or terminal fluorine atoms; since the single-bond covalent radius of molybdenum is virtually the same as that of tungsten, comparisons with molybdenum compounds are equally valid.[45] Perhaps the best comparisons are with the isoelectronic d^6 diazoalkane complex **18**, $[(CH_3COCH_2(CH_3)C{=}NN)W(diphos)_2F]^+$ (diphos = $Ph_2PCH_2CH_2PPh_2$), which has a terminal W–F bond length of 2.019 (14) Å[42a] and with a 7-coordinate tricarbonyl W(II) complex, which has a terminal W–F bond length of 2.032 (4) Å.[46] Since the W–(μ-F) interaction in **3**, **5**, and **6** is 2.17–2.19 Å, coordination of the Lewis acids SbF_5, BF_3, and PF_5 in effect only lengthens the W–F bond by ~0.15 Å. That this is a true lengthening is seen by the fact that the W–P, W–C, and W–N bond lengths are typical of other d^6 tungsten compounds.[34a,c,45] A number of high-oxidation-state tungsten and molybdenum fluorides and oxyfluorides have terminal and/or bridging fluoride ligands;[42c,47] terminal M–F bond lengths are typically ~1.80 Å, although one is 2.058 (4) Å,[47f] while bridging M–F bond lengths—all are dimeric M(μ-F)M compounds with the exception of $F_4(O)W(\mu\text{-}F)XeF$[47e]—are typically ~2.1–2.2 Å but exhibit more variability and range from 1.93 (1) to 2.31 (1) Å. The $[MoF_3O]^+$ adduct of $[SbF_6]^-$ mentioned above—better described as the chain compound $\{(\mu\text{-}F)MoF_3(O)(\mu\text{-}F)SbF_4\}_\infty$—is similar to these compounds, having terminal Mo–F bond lengths that average 1.77 (3) Å and bridging Mo–F bond lengths of 2.145 (6) and 2.210 (6) Å.[14b] One obvious conclusion is that tungsten and molybdenum bridging fluorine bond lengths are not sensitive to steric and electronic factors. Thus, any attempt to *quantify* the bond order for the W(μ-F)EF_n interaction in **3**, **5**, and **6** on the basis of a W–F single-bond length of 1.8–2.0 Å would not be meaningful. Nevertheless, in a *qualitative* sense, the fact that the W–F bond lengths in **3**, **5**, and **6** of 2.17–2.19 Å are scarcely (if at all) longer than dimeric M(μ-F)M (M = Mo, W) bond lengths suggests that the noncoordinating anions are in fact covalently bound to tungsten and that the interaction is not purely ionic. A similar conclusion was drawn for the isoelectronic compound $(CO)_5Re(\mu\text{-}F)ReF_5$, which has bridging d^6 Re–F bond lengths of 2.13 (2) and 2.20 (2) Å for the two crystallographically nonequivalent molecules that are found in the unit cell.[48] While the average bond length of 2.17 (4) Å is the same as the W–F bond lengths in **3**, **5**, and **6**, the large variability once again suggests that the M–(μ-F) bond length does not provide a quantitative guide to the strength of the M–F interaction.

Comparisons of Anion Interactions. We next turn to the structure correlation method of Bürgi and Dunitz[49] in order to attempt to analyze the strength of the interaction between the noncoordinating anion and the transition-metal cation, both in our compounds and in others for which literature data are available. Here, observation of a good correlation of Δd_M with Δd_E according to the bond-order conservation function given by eq 1[50] for systems of the form M–F–E (M = transition metal,

$$10^{-\Delta d_E/c} + 10^{-\Delta d_M/c} = 1 \qquad (1)$$

E = SbF_5, BF_3, PF_5, ReF_5) would allow the conclusion to be drawn

(45) Churchill, M. R. *Perspect. Struct. Chem.* **1970**, *3*, 91–164.
(46) Richmond, T. G.; Osterberg, C. E.; Arif, A. M. *J. Am. Chem. Soc.* **1987**, *109*, 8091–8092.
(47) (a) Edwards, A. J.; Peacock, R. D. *J. Chem. Soc.* **1961**, 4253–4254. (b) Edwards, A. J.; Peacock, R. D.; Small, R. W. H. *Ibid.* **1962**, 4486–4491. (c) Edwards, A. J.; Steventon, B. R. *J. Chem. Soc. A* **1968**, 2503–2510. (d) Bennett, M. J.; Haas, T. E.; Purdham, J. T. *Inorg. Chem.* **1972**, *11*, 207–208. (e) Tucker, P. A.; Taylor, P. A.; Holloway, J. H.; Russell, D. R. *Acta Crystallogr., Sect. B* **1975**, *B31*, 906–908. (f) Edwards, A. J.; Slim, D. R.; Guerchais, J. E.; Kergoat, R. *J. Chem. Soc., Dalton Trans.* **1977**, 1966–1968. (g) Chisholm, M. H.; Huffman, J. C.; Kelly, R. L. *J. Am. Chem. Soc.* **1979**, *101*, 7100–7104. (h) Edwards, A. J.; Slim, D. R.; Guerchais, J. E.; Kergoat, R. *J. Chem. Soc., Dalton Trans.* **1980**, 289–291. (i) Hoskins, B. F.; Linden, A.; O'Donnell, T. A. *Inorg. Chem.* **1987**, *26*, 2223–2228.
(48) Bruce, D. M.; Holloway, J. H.; Russell, D. R. *J. Chem. Soc., Dalton Trans.* **1978**, 64–67.
(49) (a) Bürgi, H. B. *Inorg. Chem.* **1973**, *12*, 2321–2325. (b) Britton, D.; Dunitz, J. D. *J. Am. Chem. Soc.* **1981**, *103*, 2971–2979. (c) Bürgi, H. B.; Dunitz, J. D. *Acc. Chem. Res.* **1983**, *16*, 153–161.
(50) Expressions in eq 1–2 and Table VII are defined as follows: c is a constant that depends on the type of bond;[49] $\Delta d_M = d[M\text{–}F_b] - d[M\text{–}F_t]$, where $d[M\text{–}F_b]$ is the observed bridging M–F bond length and $d[M\text{–}F_t]$ is the corresponding standard single-bond distance (a literature value for a terminal M–F bond length for the same oxidation state of the transition metal; see Table VII, footnote c); $\Delta d_E = d[E\text{–}F_b] - d_i[E\text{–}F_t]$, where $d[E\text{–}F_b]$ is the observed bridging E–F bond length and $d_i[E\text{–}F_t]$ is a literature value for the terminal E–F bond length in the free ion $[EF_n]^-$ ($[EF_n]^- = [SbF_6]^-$, $[BF_4]^-$, $[PF_6]^-$, $[ReF_6]^-$; see Table VII, footnote d); $d[E\text{–}F_t]$ is the observed terminal M–F bond length in the bridging anion adduct.
(51) (a) Emsley, J.; Arif, M.; Bates, P. A.; Hursthouse, M. B. *J. Chem. Soc., Dalton Trans.* **1987**, 2397–2399. (b) Edwards, A. J. *Adv. Inorg. Chem. Radiochem.* **1983**, *27*, 83–112. (c) Wyckoff, R. W. G. *Crystal Structures*, 2nd ed.; Wiley Interscience: New York, 1963; Vol. I. (d) Baur, W. H. *Acta Crystallogr.* **1958**, *11*, 488–490. (e) Anzai, K.; Hatano, K.; Lee, Y. J.; Scheidt, W. R. *Inorg. Chem.* **1981**, *20*, 2337–2339. (f) Paine, R. T.; Ryan, R. R.; Asprey, L. B. *Ibid.* **1975**, *14*, 1113–1117. (g) Levy, J. H.; Taylor, J. C.; Wilson, P. W. *J. Inorg. Nucl. Chem.* **1977**, *39*, 1989–1991. (h) Fischer, P.; Schwarzenbach, D.; Rietveld, H. M. *J. Phys. Chem. Solids* **1971**, *32*, 543–550. (i) Angoletta, M.; Bellon, P. L.; Manassero, M.; Sansoni, M. *Gazz. Chim. Ital.* **1977**, *107*, 441–442. (j) Carroll, J. A.; Cobbledick, R. E.; Einstein, F. W. B.; Farrell, N.; Sutton, D.; Vogel, P. L. *Inorg. Chem.* **1977**, *16*, 2462–2469. (k) Edwards, A. J.; Jones, G. R. *J. Chem. Soc. A* **1968**, 2511–2515. (l) Cameron, T. S.; Grundy, K. R.; Robertson, K. N. *Ibid.* **1982**, *21*, 4149–4155. (m) Horn, E.; Snow, M. R. *Aust. J. Chem.* **1984**, *37*, 35–45. (n) Hoskins, B. F.; Linden, A.; Mulvaney, P. C.; O'Donnell, T. A. *Inorg. Chim. Acta* **1984**, *88*, 217–222.
(52) (a) Caron, A. P.; Ragle, J. L. *Acta Crystallogr., Sect. B* **1971**, *B27*, 1102–1107. (b) Wang, Y.; Calvert, L. D.; Brownstein, S. K. *Ibid.* **1980**, *B36*, 1523. (c) English, R. B.; Heyns, A. M. *J. Crystallogr. Spectrosc. Res.* **1984**, *14*, 531–540. (d) Kruger, G. J.; Pistorius, C. W. F. T.; Heyns, A. M. *Acta Crystallogr., Sect. B* **1976**, *B32*, 2916–2918. (e) Brunton, G. *Ibid.* **1969**, *B25*, 2161–2162. (f) Clark, M. J. R.; Lynton, H. *Can. J. Chem.* **1969**, *47*, 2579–2586. (g) Bode, H.; Clausen, H. *Z. Anorg. Allg. Chem.* **1951**, *265*, 229–243. (h) Bode, H.; Teufer, G. *Ibid.* **1952**, *268*, 20–24. (i) Bode, H.; Teufer, G. *Ibid.* **1952**, *268*, 129–132. (j) Karlin, K. D.; Lewis, D. L.; Rabinowitz, H. N.; Lippard, S. J. *J. Am. Chem. Soc.* **1974**, *96*, 6519–6521. (k) Foxman, B. M.; Klemaczyk, P. T.; Liptrot, R. E.; Rosenblum, M. *J. Organomet. Chem.* **1980**, *187*, 253–265. (l) Head, R. A.; Hitchcock, P. B. *J. Chem. Soc., Dalton Trans.* **1980**, 1150–1155. (m) Peacock, R. D. *J. Chem. Soc.* **1957**, 467–469. (n) Kemmitt, R. D. W.; Russell, D. R.; Sharp, D. W. A. *Ibid.* **1963**, 4408–4413.
(53) Yamamoto, Y.; Aoki, K.; Yamazaki, H. *Inorg. Chim. Acta* **1982**, *68*, 75–78.
(54) Gantar, D.; Leban, I.; Friec, B.; Holloway, J. H. *J. Chem. Soc., Dalton Trans.* **1987**, 2379–2383.
(55) Edwards, A. J.; Taylor, P. *J. Chem. Soc., Chem. Commun.* **1971**, 1376–1377.
(56) Bruce, D. M.; Holloway, J. H.; Russell, D. R. *J. Chem. Soc., Dalton Trans.* **1978**, 1627–1631.

Table VII. Comparisons[a] of Bond Distances (Å) and Angles (deg) in Adducts of $[SbF_6]^-$, $[BF_4]^-$, $[PF_6]^-$, and $[ReF_6]^-$

compd[b]	d[M–F$_b$]	d[E–F$_b$]	Δd_M[c]	Δd_E[d]	d[E–F$_t$]	D_d°, %	∠(F$_b$–E–F$_t$)[e]	D_a, %	∠(M–F$_b$–E)	ref
$(en)_2Cu\{(\mu\text{-}F)BF_3\}_2$	2.56 (2)	1.38 (3)	0.651	−0.026	1.36 (5)	−1.8				5a
$[(bpy)_2Cu(\mu\text{-}F)BF_2(\mu\text{-}F)]_\infty[BF_4]$	2.61 (5)	1.38 (1)	0.705	−0.024	1.37 (1)	−1.7				4b, 5f
$(ArNC)_2Ag(\mu\text{-}F)_2PF_4$	2.67 (1)	1.56 (2)	0.200	−0.023	1.507 (2)	−1.5				53
$(Ph_3P)_3Cu(\mu\text{-}F)BF_3$	2.31 (3)	1.39 (3)	0.466	−0.015	1.35 (1)	−1.1	108.7 (4)	4	180.0	5c
$[(en)_2(H_2O)Ni(\mu\text{-}F)BF_3][BF_4]$	2.12 (2)	1.41 (1)	0.120	0.002	1.38 (1)	0.1	112.7 (18)	−16	131.8	5b
$(TPP)Fe(\mu\text{-}F)SbF_5$	2.105 (3)	1.905 (3)	0.313	0.006	1.84 (2)	0.3	89.1 (17)	6	150.4 (2)	16a
$\{(\mu\text{-}F)F_3(O)Mo(\mu\text{-}F)SbF_4\}_\infty$	2.18 (3)	1.937 (6)	0.351	0.038	1.82 (2)	2.0				14b
$F_2(O)U\{(\mu\text{-}F)SbF_5\}_2$	2.34 (2)	1.95 (2)	0.361	0.052	1.83 (2)	2.7				14a
$Ag\{(\mu\text{-}F)SbF_5\}_2$	2.11 (2)	1.95 (1)	0.043	0.055	1.836 (7)	2.9				54
$Me_2PhP(CO)_3(NO)W(\mu\text{-}F)SbF_5$ (**3b**)	2.17 (1)	1.95 (1)	0.143	0.055	1.86 (1)	2.9	87.3 (12)	18	147.2 (6)	this work
$(Ph_3P)_2(CO)(H)(Cl)Ir(\mu\text{-}F)BF_3$	2.272 (3)	1.448 (6)	0.127	0.042	1.336 (5)	3.0	108.0 (7)	8	125.7 (3)	3b
$Cy_3P(CO)_3(NO)W(\mu\text{-}F)SbF_5$ (**3c**)	2.186 (3)	1.979 (3)	0.160	0.080	1.85 (1)	4.2	86.3 (12)	25	138.9 (2)	this work
$(\eta^2\text{-}Sb_2F_{11})(O)_2U(\mu\text{-}F)SbF_5$	2.34 (1)	1.99 (1)	0.360	0.086	1.85 (1)	4.5				14c
$\{(\mu\text{-}F)F_3(O)Re(\mu\text{-}F)SbF_4\}_2$	2.16 (8)	2.00 (4)	0.293	0.102	1.83 (2)	5.4				14b
$(CO)_5Re(\mu\text{-}F)ReF_5$	2.17 (4)	1.97 (2)	0.158	0.102	1.84 (4)	5.5	88.9 (16)	7	140 (2)	48
$[F_5Sb(\mu\text{-}F)SbF_5]^-$[f]	2.02 (1)	2.02 (1)	0.120	0.120	1.84 (2)	6.3	85.5 (3)	30	160 (1)[g]	12c–i
$\{(\mu\text{-}F)F_4Sb(\mu\text{-}F)SbF_4\}_2$	2.03 (3)	2.03 (3)	0.126	0.126	1.82 (5)	6.6				55
$Me_3P(CO)_3(NO)W(\mu\text{-}F)BF_3$ (**5**)	2.168 (7)	1.50 (1)	0.142	0.094	1.36 (3)	6.7	105.7 (16)	19	128.1 (7)	this work
$[Re(CO)_6][F_5Re(\mu\text{-}F)ReF_5]$	2.009 (2)	2.009 (2)	0.146	0.146	1.84 (3)	7.8	86.8 (1)	21	180.0	56
$Me_3P(CO)_3(NO)W(\mu\text{-}F)PF_5$ (**6**)	2.19 (1)	1.73 (1)	0.161	0.148	1.57 (1)	9.3	87.1 (2)	19	142.4 (6)	this work

[a] See text, eq 1–3, and ref 50 for definitions of parameters d[M–F$_b$], d[E–F$_b$], Δd_M, Δd_E, d[E–F$_t$], D_d°, and D_a. For the angular comparisons, only the η^1-adducts are evaluated. [b] Abbreviations: bpy, 2,2′-bipyridine; en, 1,2-diaminoethane; Ar, 2,4,6-tri-*tert*-butylbenzene; TPP, *meso*-tetraphenylporphinato. [c] Values of d[M–F$_t$] and references for a given M are as follows: Cu(II), 1.909 (14) Å;[51a] Ag(I), 2.468 (1) Å;[51b] Cu(I), 1.84 Å;[51c] Ni(II), 2.002 (16) Å;[51d] (TPP)Fe^{III}, 1.792 (3) Å;[51e] Mo(VI), 1.827 (9) Å;[47c] U(VI), 1.98 (3) Å;[51f,g] Ag(II), 2.071 (3) Å;[51h] W(0), 2.026 (7) Å;[42a,46] Ir(III), 2.145 (65) Å;[51i,j] Re(VI), 1.862 (12) Å;[51k] Re(I), 2.007 (34) Å;[51l,m] Sb(V), 1.899 (10) Å;[12i] Re(V), 1.863 (4) Å.[51n] [d] Values of d_i[E–F$_t$] are as follows: Sb–F = 1.899 (10) Å;[12i] B–F = 1.406 (4) Å;[52a] P–F = 1.585 (10) Å;[52b,c] Re–F = 1.863 (4) Å.[51n] For Sb and B values are from the $[NS]^+$ and $[NH_4]^+$ salts and are corrected for thermal motion (see text); uncorrected values from the K^+ salts are 1.844 (4)[52d] and 1.384 (15) Å,[52e,f] respectively. Only uncorrected values are available for P (Cs^+ and $[NMe_4]^+$ salts) and for Re (Cs^+ salt). Since the value for P is at the long end of the range of observed values,[52g–l] it may be reasonably accurate. The Re value should probably be closer to the Sb value, on the basis of similar unit cell dimensions for their salts.[52m,n] [e] Average of three (μ-F)–B–F angles for $[BF_4]^-$ and of four (μ-F)–E–F$_{eq}$ angles for $[SbF_6]^-$, $[PF_6]^-$, and $[ReF_6]^-$. [f] Structures of this anion have been carried out with a variety of cations as the counterion.[12c–i] [g] Range of angles is 146–180°; mean is 155°.

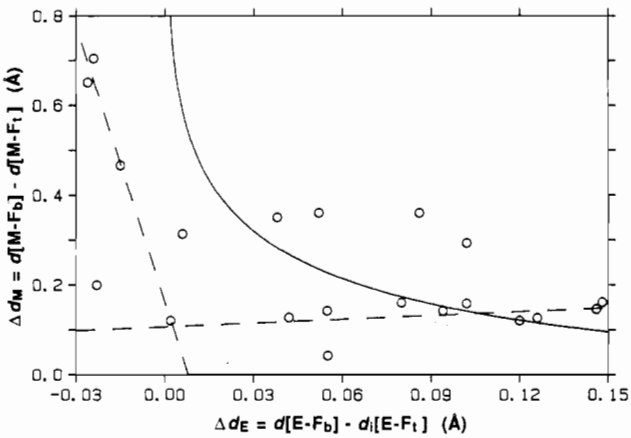

Figure 9. Plot of Δd_M vs Δd_E for the data in Table VII. The solid line is a plot of eq 1, where c = 0.4 Å.[50] Dashed lines are for illustration of the "ionic" adducts ($\Delta d_E \approx 0$ Å) and the "covalent" adducts ($\Delta d_M \approx 0.14$ Å).

that the relative strength of the M–F interaction increases as Δd_M decreases or —equivalently—as Δd_E increases. Data are collected in Table VII and plotted in Figure 9 for 20 $[SbF_6]^-$, $[BF_4]^-$, $[PF_6]^-$, and $[ReF_6]^-$ adducts, along with the terminal M–F and ionic E–F bond lengths (d[M–F$_t$] and d_i[E–F$_t$], respectively[50]) from which Δd_M and Δd_E are derived. As can be seen from Figure 9, the fit to eq 1 is not good, but since we have already noted above that tungsten- and molybdenum–fluorine bond orders are not readily quantified, the poor fit is not surprising. The plot is nevertheless instructive, since most of the adducts seem to fall into three groups: one with $\Delta d_E \sim 0$ Å consists of d^8–d^{10} adducts (Cu, Ni, Ag) that are most nearly ionic, the second with $\Delta d_M \approx 0.3$ Å consists of high-oxidation-state (+6) oxyfluoride adducts (M = Mo, Re, U), and the third with $\Delta d_M \approx 0.14$ Å consists of the low-oxidation-state adducts with π-acid ligands (M = W, Re, Ir) as well as the symmetrical antimony and rhenium fluoride compounds $(SbF_5)_4$ and $[E_2F_{11}]^-$ (E = Sb, Re). It is tempting to conclude that the first group consists of weakly interacting ionic compounds and the third group consists of strongly interacting covalent compounds. The $[SbF_6]^-$ adduct of (TPP)Fe^{III} could be considered to be a member of the second group of high-oxidation-state compounds, while $Ag\{(\mu\text{-}F)SbF_5\}_2$ does not naturally fit in any group. We conclude that a smooth correlation of the type seen in X–M···Y systems, where the ligating atoms of the X and Y groups that change are typically halides, C, N, O, or S,[49] will not be seen in comparisons involving transition metals in widely different oxidation states, although within groups of related compounds comparisons may be valid.

An alternative approach for comparison purposes is to examine only the *anion* geometry, by measuring the degree of bond length and angle *distortion* upon coordination.[14b] Our assumption is that in general, an increase in anion distortion will correlate with an increase in the strength of the interaction with the transition metal. We propose an absolute scale of anion bond length distortion, D_d° (eq 2), where d[E–F$_b$] (E = Sb, B, P, Re) is the E–F bridging

$$D_d° = \{(d[E\text{–}F_b] - d_i[E\text{–}F_t])/d_i[E\text{–}F_t]\} \times 100 \qquad (2)$$

distance and d_i[E–F$_t$] is the E–F distance in the free anions. A completely ionic complex would have D_d° = 0%, while increasingly covalent complexes would have D_d° > 0%, corresponding to the percentage increase of the length of the bridging E–F bond over that in the free anion. For completeness, we also define a scale of anion *angular* distortion, D_a (eq 3), which we will apply only

$$D_a = \{[\alpha - \angle(F_b\text{–}E\text{–}F_t)]/\beta\} \times 100 \qquad (3)$$

to the η^1-anion adducts. Here, ∠(F$_b$–E–F$_t$) is the average of the three bridging to terminal fluorine angles in $[BF_4]^-$ adducts or the four bridging to equatorial terminal fluorine angles in the octahedral $[SbF_6]^-$, $[PF_6]^-$ and $[ReF_6]^-$ adducts, α is 109.5 or 90° as appropriate, and β—representing the maximum distortion possible—is 19.5° for $[BF_4]^-$ and 15° for $[SbF_6]^-$ and $[PF_6]^-$. These values for β represent the motion on going from tetrahedral $[BF_4]^-$ to planar BF_3 and from octahedral $[SbF_6]^-$ and $[PF_6]^-$ to trigonal-bipyramidal SbF_5 and PF_5. In the latter case, the 15° is the average of the 0° motion of the two equatorial fluorine atoms that become the axial atoms in the *tbp* product and the 30° motion of the two fluorine atoms that become the equatorial atoms in the *tbp* product. Our assumption is that the stronger the M–F interaction and the longer the E–F bond, the more the terminal

fluorine atoms will bend *toward* the bridging fluorine atom, as the system moves along an imaginary reaction coordinate toward the dissociated neutral species M–F and EF_n (n = 3, 5). Thus, D_a = 0% corresponds to no movement of the terminal fluorine atoms and hence a completely ionic complex, D_a = 100% corresponds to the maximum movement of the terminal fluorine atoms and hence E–(μ-F) cleavage, and an intermediate value—presumably that from $[Sb_2F_{11}]^-$ (**1**)—should correspond to the fully "covalent" adduct.

The data for eq 2 and 3 and results are collected in Table VII, where the listing is in order of increasing absolute bond length distortion D_d°. The two distortion parameters D_d° and D_a are only roughly correlated, so while they provide relatively independent evidence about the degree of anion interaction with the metal center, we will consider only the D_d° scale, since (1) the angular distortions fall in a much more restrictive range than do the bond length distortions and (2) the D_a data set is more restrictive, since only η^1-anion adducts are included. On the basis of D_d°, the bonding in the Cu, Ni, and Ag d^8–d^{10} adducts—again with the exception of $Ag\{(\mu\text{-F})SbF_5\}_2$— as well as the $[SbF_6]^-$ adduct of (TPP)Fe^{III} would be considered to be fairly ionic (D_d° = −1.8–0.3%), while a fairly uniform subsequent increase in D_d° from 2.0 to 9.3% over a range of $[SbF_6]^-$, $[BF_4]^-$, $[PF_6]^-$ and $[ReF_6]^-$ adducts suggests a corresponding range of increasingly covalent bonding. Distortion in the $[SbF_6]^-$ adducts ranges from 0.3–6.6%; this latter value must be considered to be the maximum distortion possible without actually cleaving the Sb–F bond, given that SbF_5 is the strongest Lewis acid. The low-oxidation-state tungsten $[SbF_6]^-$ adducts **3b** and **3c** therefore exhibit ~40–60% of the maximum covalent bonding interaction possible; since there are high-oxidation-state $[SbF_6]^-$ adducts with higher and lower values of D_d°, this distortion parameter is clearly not an artifact of transition-metal oxidation state, unlike the result seen above for the plot of Δd_M vs Δd_E (Figure 9). While there are only two data points for the $[ReF_6]^-$ adducts, the 7.8% distortion seen in $[Re_2F_{11}]^-$ must again be considered to be the maximum value possible, so the 5.5% distortion in the $[ReF_6]^-$ adduct with $[(CO)_5Re]^+$ is ~70% of the maximum and is in fact quite high. In considering the $[BF_4]^-$ and $[PF_6]^-$ adducts, while a wide range of interactions is seen, there is no way to know the "maximum" distortion with any certainty, since structures of covalent adducts analogous to $(SbF_5)_4$, $[Sb_2F_{11}]^-$, and $[Re_2F_{11}]^-$ are unknown.

While our basic assumption is that an increase in anion distortion—that is, D_d°—will correlate with an increase in the strength of the interaction with the transition metal, the above data suggests that *different anions undergo different degrees of distortion upon achieving the same degree of interaction with a metal cation.* We draw this inference from the different *maximum* distortions for $[SbF_6]^-$ (D_d° = 6.6%) and $[ReF_6]^-$ (D_d° = 7.8%) and from the *different* distortions for **3b** (D_d° = 2.9%), **5** (D_d° = 6.7%), and **6** (D_d° = 9.3%). In these latter three tungsten compounds, we assume that similar degrees of interaction with tungsten exist, at least to a first approximation: these adducts are essentially isostructural, have similar W–F bond lengths, and are of *broadly* similar stability. It should be noted that we do not include Cy_3P adduct **3c**, since due to steric hindrance it would not be reasonable to assume the same degree of interaction. A more quantitative view of the meaning of the $[BF_4]^-$ and $[PF_6]^-$ distortion values—that is, the degrees of interaction to a *second* approximation—would be available if geometries for the maximally distorted species $[F_3B(\mu\text{-F})BF_3]^-$ and $[F_5P(\mu\text{-F})PF_5]^-$ were available. While structural data does not exist, MNDO calculations on $[F_3B(\mu\text{-F})BF_3]^-$ give a bridging B–F bond length of 1.462 Å, and Xα calculations involving $[F_5P(\mu\text{-F})PF_5]^-$ use a bridging P–F bond length of 1.73 Å.[57] We suggest an independent estimate of the bridging bond lengths as follows. The sum of the single-bond covalent radii[58] for the Sb–F bond is 2.00 Å, which is similar to the "covalent" Sb–(μ-F) bond length of ~2.02 Å seen in the maximally distorted species $(SbF_5)_4$ and $[Sb_2F_{11}]^-$, and ~0.10 Å greater than the observed "ionic" Sb–F bond length in $[SbF_6]^-$. The sums of the single-bond covalent radii for the B–F and P–F bonds are 1.53 and 1.74 Å, respectively, which are ~0.12 Å and ~0.16 Å greater than their observed ionic radii in the free anions. Given the facts that (1) the *calculated* covalent E–F bond lengths are consistently ~0.13 (2) Å greater than the *observed* ionic E–F bond lengths and (2) the *calculated* Sb–F bond length is just shorter than the *observed* bond length for the maximally distorted adducts of $[SbF_6]^-$, we suggest that the same is true for the B–F and P–F bond lengths: *maximally distorted adducts of $[BF_4]^-$ and $[PF_6]^-$ should exhibit B–F and P–F bond lengths comparable to their calculated covalent values of 1.53 and 1.74 Å—values similar to the MNDO and Xα values of 1.46 and 1.73 Å.* This leads to the remarkable conclusion that *the $[BF_4]^-$ and particularly the $[PF_6]^-$ adducts **5** and **6** are near to the maximum degree of distortion possible.* Any further distortion would simply lead to B–F or P–F cleavage—that is, fluoride abstraction by the transition-metal Lewis acid—and both reactions are well-known.[4m,5g,h,42,51i,j,l,59] Thus, we claim that $[SbF_6]^-$ is a *better* ligand since *substantially* less distortion—hence less energy— is required for coordination to take place. On the basis of the above approximation of the maximum distortion possible for $[BF_4]^-$ and $[PF_6]^-$, these must be considered to be comparable ligands, although, from the experimental point of view, the $[BF_4]^-$ adduct **5** is unambiguously more stable than the $[PF_6]^-$ adduct **6**.

Nature of the Fluorine Bridge. Examination of intra- and intermolecular carbonyl C–F and C–O nonbonding distances in **3b**, **3c**, **5**, and **6** reveals many short contacts of 2.82–~3.3 Å; contacts of ≤3.10 Å are listed in Table VIII. The existence of such nonbonding distances is surprising, since the sum of the van der Waals radii for fluorine and the carbonyl carbon is at least 3.1 Å.[60] Clearly, these molecules are relatively crowded; for instance in each case one of the phosphine alkyl groups nearly eclipses the W–F bond (Table VIII), suggesting that the linear nitrosyl ligand provides more steric hindrance than does the anion, which of course can bend away from the phosphine ligand. One could propose that the W–F interaction is impressively strong and so these short contacts are present *despite* the crowding or that there is an *attractive* interaction between the fluorine and carbonyl carbon and oxygen atoms—for carbon perhaps due to fluorine lone-pair donation into the CO π^* orbital and for oxygen perhaps due to simple electrostatic attraction. While such an O–F interaction is reasonable, C–F bonding might be expected to result in lengthening of the E–F bonds (E = Sb, P, B) and in bending of the W–C–O angles from 180°, with the oxygen in particular pushed away from the interacting fluorine atom. No consistent patterns are observed—that is, bond length differences are insignificant and oxygen is bent both toward and away from the interacting fluorine atom, as measured by the deviation of the *sum* of the F–C–W and F–C–O angles from 180°. Nevertheless, while the $[BF_4]^-$ adduct **5** and the $[PF_6]^-$ adduct **6** *necessarily* must have

(57) For $[F_3B(\mu\text{-F})BF_3]^-$ the calculation indicates the anion should be bound and also gives a relatively short terminal B–F bond length of 1.373 Å,[57a] while for $[F_5P(\mu\text{-F})PF_5]^-$ the origin of the geometry—which again involved a relatively short terminal P–F bond length of 1.55 Å—was not explicitly described;[57b] see: (a) Cuthbertson, A. F.; Glidewell, C.; Liles, D. C. *J. Mol. Struct.* **1982**, *87*, 273–282. (b) Gutsev, G. L.; Boldyrev, A. I. *Chem. Phys. Lett.* **1984**, *108*, 250–254.

(58) Standard single-bond covalent radii are as follows: F, 0.64 Å; Sb, 1.36 Å; B, 0.89 Å; P, 1.10 Å. See: (a) Bondi, A. *J. Phys. Chem.* **1964**, *68*, 441–451. (b) Alcock, N. W. *Adv. Inorg. Chem. Radiochem.* **1972**, *15*, 1–58.

(59) (a) Marks, T. J.; Seyam, A. M. *Inorg. Chem.* **1974**, *13*, 1624–1627. (b) Snow, M. R.; Wimmer, F. L. *Aust. J. Chem.* **1976**, *29*, 2349–2361. (c) Raab, K.; Beck, W. *Chem. Ber.* **1985**, *118*, 3830–3848. (d) Jordan, R. F.; Dasher, W. E.; Echols, S. F. *J. Am. Chem. Soc.* **1986**, *108*, 1718–1719. (e) Ellis, R.; Henderson, R. A.; Hills, A.; Hughes, D. L. *J. Organomet. Chem.* **1987**, *333*, C6–C10.

(60) Standard values for the van der Waals radius of fluorine range from 1.35 to 1.50 Å (the lower estimate may be the most appropriate here, since it is equal to the ionic radius of F^-); in addition, for C–F a nonspherical shape is seen with shorter contacts (1.30 Å) allowed at a C–F···X angle of !80°, but 1.38 Å at 90°.[60b] Values for the van der Waals radius for the carbonyl ligand in the range of aromatic and acetylenic radii, 1.72–1.80 Å, are reasonable, with the best value taken to be 1.77 Å. See ref 58 and: (a) Pauling, L. *The Nature of the Chemical Bond*, 3rd ed.; Cornell University Press: Ithaca, NY, 1960; pp 257–264. (b) Nyburg, S. C.; Faerman, C. H. *Acta Crystallogr., Sect. B* **1985**, *B41*, 274–279.

Table VIII. Other Comparisons of X-Ray Data for **3-6**: Geometry Related to the W-(μ-F) Bond and Intra- and Intermolecular Fluorine-Carbon and Fluorine-Oxygen CO Contacts to 3.10 Å

compd	∠(C-P-W-F_b)[a]	∠(P-W-F_b-E)[b]	F(2) intra	F(2) inter	F(3) intra	F(3) inter	F(4)[c] inter	F(5)[c] inter	F(6)[c] inter
$Me_2PhP(CO)_3(NO)W(\mu\text{-}F)SbF_5$ (**3b**)	4.1	139.0	C(3), 3.03	O(3), 2.91	none	O(1), 2.97 C(1), 3.07	none	C(2), 3.10	none
$Cy_3P(CO)_3(NO)W(\mu\text{-}F)SbF_5$ (**3c**)	10.9	167.0	C(1), 3.00	none	C(1), 3.08	none	none	O(2), 2.82	none
$Me_3P(CO)_3(NO)W(\mu\text{-}F)BF_3$ (**5**)	9.5	161.3	none O(3), 2.94	C(3), 2.93 O(1), 3.10 C(1), 3.09	C(1), 2.88	none	O(3), 3.09	none	none
$Me_3P(CO)_3(NO)W(\mu\text{-}F)PF_5$ (**6**)	0.8	145.9	C(3), 2.93	none	C(1), 2.97	none	C(1), 2.93 O(1), 2.95	C(2), 2.84 O(2), 2.98	O(3), 2.99

[a] Torsion angle in degrees; C is the eclipsing phosphine alkyl substituent. [b] Torsion angle in degree; E = Sb, B, P(2). [c] No short intramolecular contacts (<3.15 Å) are present.

a number of geometrical differences from the $[SbF_6]^-$ adducts—for instance due to the tetrahedral anion geometry of **5** and the B-F and P-F bond lengths of **5** and **6** that are shorter than the Sb-F bond lengths of **3b** and **3c**—in both cases the observed W-(μ-F)-E angles (Table VII) and P-W-(μ-F)-E torsional angles (Table VIII) combine to result in surprisingly *similar* nonbonding C-F and O-F distances. The differences are particularly obvious in **5**, where for instance the tetrahedral $[BF_4]^-$ anion ought to provide less hindrance to the carbonyl ligand trans to the phosphine, and consistent with this the P-W-F-B torsional angle is 161.3°. However, the W-(μ-F)-B angle of 128° is much more acute than the corresponding angles in **3b**, **3c**, and **6**, thereby yielding similar C-F distances *despite* all of the geometric differences noted above. We therefore conclude that rather than being energetically *un*favorable, some aspect of the overall geometry that yields the short contact distances must be energetically *favorable*.

In the absence of an obvious attractive C-F interaction, the controlling factor might be due to W-(μ-F)-E *angle strain*. Crabtree has pointed out that linear angles are often seen in electron-deficient compounds, which can be interpreted to indicate the presence of π bonding.[42c] However, nonlinear angles in the 140-150° range are not that uncommon in electron-deficient compounds,[14,47c,e,i] and Peacock has suggested that metal-fluorine bonds are too long for π bonding.[61] We note that all of the compounds used to make generalizations about π bonding consist of *octahedrally* coordinated fragments bridged by fluorine and/or have only electronegative oxide and fluoride ligands. Thus, steric hindrance and electrostatic repulsion can serve to give large angles about the μ-F ligand, without the intervention of π bonding. The only compounds described above that have a single fluorine bridge and that have one fragment that is *not* octahedral are those with coordinated $[BF_4]^-$, and in these cases the M-F-B angle is typically ~130°,[3b,4b,5a,b,f] the one exception ($(Ph_3P)_3Cu(\mu\text{-}F)BF_3$, Cu-F-B = 180°) is a consequence of the presence of three Ph_3P ligands (Table VII).[5c] Thus, we suggest that *the optimal M-F-E angle is closer to 90°* and that the observed angle simply reflects the steric and electrostatic repulsion of the ligands on the bridged atoms. For the octahedral species, angles greater than ~140° are expected,[14,47,48] while the presence of one sterically less encumbered tetrahedral moiety allows angles as acute as 126°.[3b] Further support for this hypothesis comes from the structure of $[Cs][Sb_2F_7]$, in which the anion is made up of two SbF_3 moieties joined by a fluoride bridge; the Sb-F-Sb angle is 125°. The authors noted the lack of any obvious stereochemical feature—the geometry at antimony was considered to be a distorted trigonal bipyramid, with the antimony lone pair in the equatorial plane—that should result in the bent fluorine bridge and concluded that the bonding fluorine orbitals were primarily p orbitals.[62] In fact, many *theoretical* studies,[63] motivated by the observation of unusual fluorine spin-spin coupling constants, have reached the conclusion that the fluorine contribution to E-F σ bonds is nearly a *pure* 2p orbital. This result is due to the large energy gap in fluorine 2s and 2p atomic orbitals, so the extent of hybridization is expected to be small (<5% s character, for instance, for C-F bonds in particular[63a,c]). In conclusion, while the questions raised concerning the dependence of the anion geometry in **3**, **5**, and **6** on an attractive C-F interaction versus the optimal hybridization about the μ-F ligand cannot be definitively resolved, it is our hypothesis that bonding primarily involving the p orbitals on the bridging fluorine atom controls the observed angles in adducts of noncoordinating fluoro anions.

Thermal Motion Analysis. In this paper we are concerned with the detailed analysis of bond lengths, yet it is well-known that the *thermal motion* of atoms in a molecule in a crystal will result in observed interatomic distances that are usually *shorter*—but never longer—than the actual distances.[64] Corrections to bond distances may be made on the basis of *assuming* certain correlations between the motions of the atoms and then examining the consequences of the model chosen to determine whether or not it is reasonable. For instance, in the widely used riding model[12i,16a,64c] a *terminally bound* light atom "rides" on a heavy atom. While the difference in atomic weights of antimony and fluorine makes it reasonable to apply this model to the $[SbF_6]^-$ adduct **3c**, where the five terminal fluorine atoms are assumed to ride on antimony, it cannot be used for $[BF_4]^-$, since the fluorine atoms are *heavier* than the boron atom and so certainly cannot be considered to ride on it, while in $[PF_6]^-$ the atomic weight difference between phosphorus and fluorine is too small—usually the correction is applied to hydrogen riding on carbon.[64a] Another limitation is that the accuracy of this model cannot be independently assessed,[65] and while the terminal Sb-F bond length corrections may be appropriate, it gives no corrections to the more interesting bridging bond lengths and no further insight into the thermal motion of the anion. For these reasons we will describe here results using an alternative model that allows for internal motion of an attached rigid group (ARG)—that is, a group of atoms that exhibits librational motion (rotational oscillation) independent of the rest of the presumably rigid molecule;[64e-g] due to this independent motion the ARG is alternatively referred to in the literature as a "nonrigid group". We note that we can consider only **3c**, **5**, and **6** because the calculations[65] require the use of anisotropic temperature parameters from the X-ray analysis; as described in the Experimental Section, these are not available for **3b**.

(61) Peacock, R. D. *Adv. Fluorine Chem.* **1973**, *7*, 113-145.
(62) Ryan, R. R.; Mastin, S. H.; Larson, A. C. *Inorg. Chem.* **1971**, *10*, 2793-2795.
(63) (a) Anderson, D. H.; Frank, P. J.; Gutowsky, H. S. *J. Chem. Phys.* **1960**, *32*, 196-204. (b) Jameson, C. J.; Gutowsky, H. S. *Ibid.* **1969**, *51*, 2790-2803. (c) Konishi, H.; Morokuma, K. *J. Am. Chem. Soc.* **1972**, *94*, 5603-5612. (d) Mallory, F. B. *Ibid.* **1973**, *95*, 7747-7752. (e) Shustorovich, E.; Dobosh, P. A. *J. Magn. Reson.* **1980**, *39*, 79-99. (f) Shustorovich, E.; Dobosh, P. A. *Ibid.* **1980**, *39*, 101-117.
(64) (a) Johnson, C. K. In *Crystallographic Computing*; Ahmed, F. R., Ed.; Munksgaard: Copenhagen, 1970; pp 207-226. (b) Trueblood, K. N. *J. Mol. Struct.* **1985**, *130*, 103-115. (c) Busing, W. R.; Levy, H. A. *Acta Crystallogr.* **1964**, *17*, 142-146. (d) Schomaker, V.; Trueblood, K. N. *Acta Crystallogr., Sect. B* **1968**, *34B*, 63-76. (e) Dunitz, J. D.; White, D. N. J. *Acta Crystallogr., Sect. A* **1973**, *29A*, 93-94. (f) Trueblood, K. N. *Ibid.* **1978**, *34A*, 950-954. (g) Schomaker, V.; Trueblood, K. N. *Ibid.* **1984**, *40 Supplement*, C-339.
(65) The thermal motion analysis was carried out by using the computer program THMA 11, originally written by E. Huber-Buser and extensively revised by K. N. Trueblood. The motions are calculated from a least-squares fit to all of the observed individual anisotropic vibration parameters (U_{ij}) in the temperature factor expression, giving a quantitative measure (R_w in footnote *h*, Table IX) of the fit of the calculated to observed U_{ij} values.

Table IX. Corrections for Thermal Motion to Fluorine Bond Lengths (Å) for **3c**, **5**, **6**, and **19**

compd[a]	bond	uncor	libration axis for attached rigid group[b]		
			W–F_b[c]	F_b–E[d]	[W–F_b] × [F_b–E][e]
$Cy_3P(CO)_3(NO)W(\mu\text{-}F)SbF_5$ (**3c**)	F(1)–W	2.186	2.189	2.188	2.189
	F(1)–Sb	1.979	1.990	1.980	1.985
	F(2)–Sb	1.868	1.880	1.894	1.872
	F(3)–Sb	1.855	1.873	1.882	1.858
	F(4)–Sb	1.858	1.877	1.885	1.860
	F(5)–Sb	1.832	1.848	1.860	1.838
	F(6)–Sb	1.857	1.868	1.858	1.862
correction[f]			0.014 (3)	0.025 (0)[g]	0.002 (1)
R_w[h]			0.135	0.114	0.192
Ω,[i] deg			8.2 (3)	9.5 (3)	3.8 (6)
$Me_3P(CO)_3(NO)W(\mu\text{-}F)BF_3$ (**5**)	F(1)–W	2.168	2.173	2.173	2.173
	F(1)–B	1.500	1.514	1.504	1.507
	F(2)–B	1.386	1.391	1.390	1.390
	F(3)–B	1.373	1.389	1.377	1.375
	F(4)–B	1.316	1.333	1.321	1.320
correction			0.010 (5)	0.001 (0)	0.001 (1)
R_w			0.102	0.118	0.130
Ω, deg			8.3 (6)	2.7 (20)	3.1 (16)
$Me_3P(CO)_3(NO)W(\mu\text{-}F)PF_5$ (**6**)	F(1)–W	2.187	2.190	2.189	2.190
	F(1)–P	1.733	1.742	1.735	1.738
	F(2)–P	1.574	1.588	1.592	1.580
	F(3)–P	1.585	1.602	1.602	1.588
	F(4)–P	1.550	1.568	1.568	1.554
	F(5)–P	1.569	1.584	1.586	1.574
	F(6)–P	1.567	1.575	1.569	1.572
correction			0.012 (3)	0.015 (0)[g]	0.002 (1)
R_w			0.127	0.127	0.170
Ω, deg			8.2 (4)	7.9 (4)	3.3 (10)
$(Ph_3P)_2(CO)(H)(Cl)Ir(\mu\text{-}F)BF_3$ (**19**)	F(1)–Ir	2.272	2.279	2.278	2.280
	F(1)–B	1.448	1.471	1.453	1.461
	F(2)–B	1.329	1.336	1.406	1.339
	F(3)–B	1.340	1.367	1.417	1.343
	F(4)–B	1.339	1.364	1.418	1.347
correction			0.016 (9)	0.075 (1)	0.004 (2)
R_w			0.093	0.084	0.116
Ω, deg			11.0 (17)	20.2 (10)	5.7 (37)

[a] The number of atoms used for calculations was as follows: **3c**, 35 (all except hydrogen); **5**, 18 (all except hydrogen); **6**, 20 (all except hydrogen); **19**, 17 (all except hydrogen and phenyl carbons not attached to phosphorus). [b] Correction assuming an attached rigid group (ARG) librates independently of the remainder of the molecule; correction is the sum of the rigid body and attached rigid group corrections.[64e-g] [c] ARG[b] is SbF_5, BF_3, or PF_5 (terminal fluorine atoms). [d] ARG[b] is effectively the same as in footnote c, but computationally it is F_5 or F_3 as appropriate. [e] Axis is the vector product of the W–F(1) and F(1)–E axes. [f] Average correction (Å) for the three (B) or five (Sb, P) E–F_t bond lengths. [g] Since ∠F(1)–E–F(6) ≈ 180°, the E–F(6) correction should be (and is) ~0 Å. The average correction is for the other four terminal fluorine bond lengths. [h] $R_w = [\sum w_{ij}(U(\text{obs})_{ij} - U(\text{calc})_{ij})^2/\sum w_{ij}U(\text{obs})_{ij}^2]^{1/2}$, $w_{ij} = 1/\sigma_{ij}$.[64d] [i] The rms librational amplitude about the ARG[b] rotation axis.

We have examined the librational motion of the $[SbF_6]^-$, $[BF_4]^-$, and $[PF_6]^-$ ions with respect to three rotational axes, namely, the W–F_b axis, the F_b–E axis, and an axis through F_b that is the vector product of the W–F_b and F_b–E axes (that is, mutually perpendicular to these two axes), as illustrated for the W–F–SbF_5 fragment:

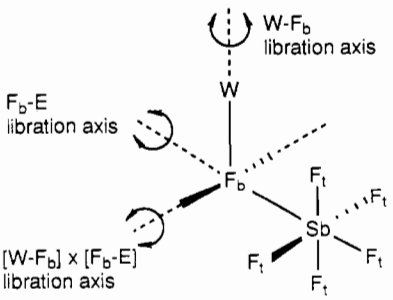

It should be noted that the bond length for the axis-defining atoms is *not* corrected, so d[W–F_b] is not affected by thermal motion of (for instance) the SbF_5 moiety, and for libration of the SbF_5 group about the F_b–Sb axis only the d[Sb–F_t] values and *not* d[Sb–F_b] will be corrected. Furthermore, for both $[SbF_6]^-$ and $[PF_6]^-$, the axial fluorine atom F(6) is virtually on the libration axis, so no correction would be expected. In addition to the bond length corrections, the attached rigid group analysis gives an angular measure of the librational motion about the proposed rotational axis; reported values for the calculated root-mean-square amplitude, Ω, range from 2–25°.[64e,f]

The results collected in Table IX show that the bridging fluorine bond lengths d[E–F_b] and d[W–F_b] are scarcely changed for any of the motions; the largest corrections are ~0.01 Å in d[E–F_b] for libration about the W–F_b axis in **3c**, **5**, and **6**. For the terminal fluorine bond lengths d[E–F_t], libration about the [W–F_b] × [F_b–E) axis results in corrections that are insignificant (~0.002 Å), and this is also reflected in the failure to achieve a better fit of calculated to observed U_{ij} parameters, as measured by the slight decreases in the residuals R_w. For libration about the W–F_b or F_b–E axes, however, significant corrections are observed.[66] Thus, for $[SbF_6]^-$ adduct **3c**, libration about the W–F_b axis yields an average 0.014-Å correction, a drop in R_w from 0.199 to 0.135, and a librational amplitude Ω = 8.2 (3)°, while libration about the F_b–Sb axis yields a larger correction of 0.025 Å—but only for the four equatorial fluorine atoms, as expected—an even bigger decrease in R_w to 0.114, and a correspondingly larger librational amplitude Ω = 9.5 (3)°. Essentially similar librational motions are calculated for $[PF_6]^-$ adduct **6**, which like **3c** contains an octahedral anion. For $[BF_4]^-$ adduct **5**, however, a different result is seen: essentially no libration about the F_b–B axis occurs (Ω = 2.7 (20)°, bond length correction averages 0.001 Å), but sig-

(66) It has proven computationally impossible to combine the two librational motions to yield a single correction (and what might prove to be somewhat smaller librational amplitudes on one or the other axis), since if there are not at least two atoms not common to both ARG's, a singular matrix arises: Trueblood, K. N. Personal Communication.

nificant libration about the W–F_b axis remains (Ω = 8.3 (6)°, bond length correction averages 0.01 Å). We presume that the change is a consequence of the tetrahedral anion geometry, since the extent of steric crowding as judged by the nonbonded contacts (Table VIII) seems comparable to that in **3c** and **6**.

The major conclusion from the thermal motion analysis is that the most interesting bond distances, those involving the bridging fluorine atom, are essentially unchanged by any librational motion of the EF_n (n = 3, 5) moiety. Such a result is not entirely unexpected, since the bridging fluorine atom is anchored to the transition metal; motion of the terminal fluorine atoms can be much greater and result in significant shortening of observed bond lengths. In order to further test this hypothesis, the terminal fluorine bond lengths in Table VII were examined. One compound stands out, namely the low-oxidation-state iridium $[BF_4]^-$ adduct **19**,[3b] where the average B–F_t bond length of 1.336 (5) Å is ~0.07

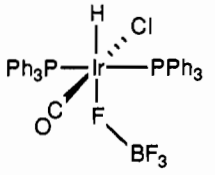

19

Å shorter than that in free $[BF_4]^-$. We were interested to determine whether, in such an extreme case, corrections for thermal motion would significantly lengthen the terminal bond lengths but still leave the bridging distances unchanged. The structure determination itself is of high quality (R_w = 0.033), but since it was carried out at room temperature, a high degree of thermal motion could be present. The results of our analysis[67] are collected in Table IX. As with the tungsten compounds, libration of BF_3 about the [Ir–F_b] × [F_b–B] axis results in essentially no bond length corrections. Libration about the Ir–F_b axis results in modest bond length corrections (0.016 (9) Å) and a substantial librational amplitude (Ω = 11 (2)°), but the libration about the F_b–B axis, Ω = 20 (1)°, is enormous, as is the average bond length correction of 0.075 (1) Å. The average corrected B–F_t bond length of 1.414 (5) Å is in accord with that of 1.406 (4) Å for free $[BF_4]^-$, where the latter value is also corrected for thermal motion.[52a] Despite these large changes, however, the Ir–F_b bond length is essentially unchanged and the F_b–B bond length correction is at most ~0.02 Å.

In summary, the above data on **3c**, **5**, **6**, and **19** demonstrate in a quantitative manner that complexation of $[SbF_6]^-$, $[BF_4]^-$, and $[PF_6]^-$ has the effect of suppressing the thermal librational motion of the bridging fluorine atom, resulting in fairly accurate *uncorrected* M–F_b and F_b–E bond lengths even when, as in **19**, substantial librational motion gives relatively *inaccurate* uncorrected E–F_t bond lengths. The same effect is present in **3c**, **5**, and **6**, but it is minimized due to the fact that our X-ray data were collected at low temperature (−140 °C), where thermal motion is expected to be relatively small. With one exception[16a] reported distances in other adducts of noncoordinating anions are uncorrected, so comparisons involving *terminal* fluorine bond lengths in general will not be valid. Nevertheless, the results presented above provide the first quantitative data that show that comparisons of the *uncorrected bridging* fluorine bond lengths *are* valid.

Conclusion

We began this paper by describing what is likely to be behind the common view that $[SbF_6]^-$ is the least coordinating of the simple "noncoordinating" anions. The most graphic illustration must be considered to be the fact that $[SbF_6]^-$ but not $[BF_4]^-$ or $[PF_6]^-$ can serve as the noncoordinating counterion for carbocations. However, this is likely to be a consequence of the much greater fluoride affinity of SbF_5 compared to that of BF_3 or PF_5[11b,44,68] and likely has nothing to do with $[BF_4]^-$ or $[PF_6]^-$ being more "coordinating" than $[SbF_6]^-$ but rather with the fact that carbocations would be expected to abstract fluoride from $[BF_4]^-$ and $[PF_6]^-$. From the inorganic point of view, the evidence is overwhelming that $[SbF_6]^-$ is a better ligand than $[BF_4]^-$ or $[PF_6]^-$. For instance, in the course of the above discussion we have listed four high-oxidation-state transition-metal oxyfluoride adducts of $[SbF_6]^-$, two silver adducts of $[SbF_6]^-$, the SbF_5 adduct of $[SbF_6]^-$ (that is, $[Sb_2F_{11}]^-$), and $(SbF_5)_4$, in which one might consider $[SbF_6]^-$ to be coordinated to $[SbF_4]^+$. Many more compounds are known that exhibit varying degrees of interaction with $[SbF_6]^-$,[69] and in fact large numbers of antimony–fluorine *chain* compounds that possess fluorine bridges are known and have been characterized by NMR spectroscopy[11c,12a,b,70] and X-ray diffraction.[62,71] None of these structures have any well-characterized analogy in boron or phosphorus fluoride chemistry,[71a] although some evidence exists for transient formation of $[P_2F_{11}]^-$ and more long-lived $[F_5P(\mu\text{-}F)SbF_5]^-$, $[B_2F_7]^-$ and $[B_3F_{10}]^-$.[44,57a,68b,72] We presume that the reason for this effect lies simply with the greater Lewis acidity of SbF_5 compared to BF_3 and PF_5, in that the latter two compounds are not acidic enough to tightly bind a fluorine atom that is already bound to another Lewis acid center. The underlying reason for this lower acidity is presumably due to the *covalent* nature of the B–F and P–F bonds compared to the *ionic* nature of the Sb-F bonds: small nonmetallic elements such as boron and phosphorus typically yield directional covalent bonds that are weaker than the ionic bonds in more metallic elements such as antimony and bismuth.[73] The ionic nature of the bonding in $[SbF_6]^-$ also would be expected to allow a greater buildup of charge on the fluorine atoms, which would make the anion a better donor ligand. Direct support for this effect comes from ab initio MO calculations: although the difference is not large, each fluorine atom is computed to have a net charge of −0.25 and −0.22 for $[SbF_6]^-$ and $[PF_6]^-$, respectively.[74]

In conclusion, both from the experimental point of view, where the $[SbF_6]^-$ and $[BF_4]^-$ adducts **3** and **5** are unambiguously more stable than the $[PF_6]^-$ adduct **6**, and from the detailed structural point of view, on the basis of our distortion parameter D_d°, the order of ligand binding strength is $[SbF_6]^- > [BF_4]^- > [PF_6]^-$.

(67) The published form of the anisotropic temperature factor expression[3b] apparently incorporates a nonstandard set of anisotropic vibrational parameters (B_{ij}'s), which we have converted according to $B_{ij} = 8\pi^2 U_{ij}$, where the form of this equation is taken from $B_{iso} = 8\pi^2\langle U^2\rangle$; see: Stout, G. H.; Jensen, L. H. *X-ray Structure Determination*; The Macmillan Co.: New York, 1968; p 449–450.

(68) (a) Olah, G. A.; Kuhn, S. J.; Tolgyesi, W. S.; Baker, E. B. *J. Am. Chem. Soc.* **1962**, *84*, 2733–2740. (b) Haartz, J. C.; McDaniel, D. H. *Ibid.* **1973**, *95*, 8562–8565. (c) Larson, J. W.; McMahon, T. B. *Ibid.* **1985**, *107*, 766–773. (d) O'Keefe, M. *Ibid.* **1986**, *108*, 4341–4343.

(69) (a) Boldrini, P.; Gillespie, R. J.; Ireland, P. R.; Schrobilgen, G. J. *Inorg. Chem.* **1974**, *13*, 1690–1694. (b) Passmore, J.; Richardson, E. K.; Whidden, T. K.; White, P. S. *Can. J. Chem.* **1980**, *58*, 851–857. (c) Birchall, T.; Myers, R. D. *Inorg. Chem.* **1981**, *20*, 2207–2211. (d) Passmore, J.; Sutherland, G.; Taylor, P.; Whidden, T. K.; White, P. S. *Ibid.* **1981**, *20*, 3839–3845. (e) Ardon, M.; Bino, A.; Cotton, F. A.; Dori, Z.; Kaftory, M.; Kolthammer, B. W. S.; Kapon, M.; Reisner, G. *Ibid.* **1981**, *20*, 4083–4090. (f) Edwards, A. J.; Khallow, K. I. *J. Chem. Soc., Chem. Commun.* **1984**, 50–51.

(70) Dean, P. A. W.; Gillespie, R. J. *J. Am. Chem. Soc.* **1969**, *91*, 7260–7264.

(71) See for instance: (a) Simons, J. H. In *Fluorine Chemistry*; Simons, J. H., Ed.; Academic Press: New York, 1964; Chapter 1. (b) Edwards, A. J.; Slim, D. R. *J. Chem. Soc., Chem. Commun.* **1974**, 178–179. (c) Gillespie, R. J.; Kent, J. P.; Sawyer, J. F.; Slim, D. R.; Tyrer, J. D. *Inorg. Chem.* **1981**, *20*, 3799–3812. (d) Nandana, W. A. S.; Passmore, J.; Swindells, D. C. N.; Taylor, P.; White, P. S.; Vekris, J. E. *J. Chem. Soc., Dalton Trans.* **1983**, 619–625. (e) Boldrini, P.; Brown, I. D.; Collins, M. J.; Gillespie, R. J.; Maharajh, E.; Slim, D. R.; Sawyer, J. F. *Inorg. Chem.* **1985**, *24*, 4302–4307. (f) Collins, M. J.; Gillespie, R. J.; Sawyer, J. F.; Schrobilgen, G. J. *Ibid.* **1986**, *25*, 2053–2057.

(72) (a) Brownstein, S.; Paasivirta, J. *Can. J. Chem.* **1965**, *43*, 1645–1649. (b) Harris, J. J. *Inorg. Chem.* **1966**, *5*, 1627–1629. (c) Burchill, P. J.; Brownstein, S.; Eastham, A. M. *Can. J. Chem.* **1967**, *45*, 17–20. (d) Brownstein, S.; Bornais, J. *Ibid.* **1968**, *46*, 225–228.

(73) (a) West, A. R. *Solid State Chemistry and its Applications*; Wiley: Chichester, England, 1984; Chapter 8. (b) Wells, A. F. *Structural Inorganic Chemistry*, 5th ed.; Clarendon Press: Oxford, 1986; Chapters 9, 19, 20, 24.

(74) Teramae, H.; Tanaka, K.; Yamabe, T. *Solid State Commun.* **1982**, *44*, 431–434.

In particular, we find that the distortion of the $[SbF_6]^-$ ligand upon coordination to the tungsten nitrosyl cation is only ~50% of the maximum distortion seen upon coordination to SbF_5, arguably the strongest Lewis acid known. However, we find that the distortion of the $[BF_4]^-$ and $[PF_6]^-$ ligands upon coordination to the tungsten nitrosyl cation is comparable to what we estimate to be the maximum distortion possible. Fortuitously, then, the $[Me_3P(CO)_3(NO)W]^+$ fragment is likely to be the strongest Lewis acid that will bind these two anions without abstraction of fluoride ion. *This result alone suggests that $[SbF_6]^-$ should be the anion of choice in the synthesis of reactive yet isolable cationic Lewis acids.* Far from yielding less stable compounds, the use of $[SbF_6]^-$ as a *coordinating* anion should yield *more* stable compounds that will still retain substitutional lability[27a] and catalytic activity.[23] All of our evidence suggests that this somewhat unconventional ordering of anion donor strength will be a general phenomenon.

Experimental Section

All manipulations of air-sensitive compounds were carried out either in a Vacuum Atmospheres inert-atmosphere glovebox under recirculating nitrogen or with standard Schlenk techniques. NMR spectra were recorded on JEOL FX90Q and Bruker WP-200, AM-360, and AM-500 spectrometers; chemical shifts are reported relative to residual $CHDCl_2$ (^1H, δ 5.32) in CD_2Cl_2 (^{13}C, 53.8 ppm), 8.5% H_3PO_4 in a 1-mm coaxial tube (^{31}P, 0.00 ppm) or internal $Me_3PW(CO)_5$ (^{31}P, −38.03 ppm in CD_2Cl_2), and external $CFCl_3$ (^{19}F, 0.00 ppm). A complete listing of ^{31}P NMR data is given in ref 27a. Infrared spectra were obtained in CH_2Cl_2 in 0.1-mm NaCl solution cells on a Perkin-Elmer 237 spectrophotometer. Elemental analyses were performed by Galbraith Laboratories, Inc., Knoxville, TN, or Desert Analytics, Tucson, AZ. Mass spectra (EI) were obtained on an AEI MS902.

All solvents were treated under nitrogen. Acetonitrile was distilled sequentially from calcium hydride and phosphorus pentoxide,[21] methylene chloride and 1,1,2-trichlorotrifluoroethane were distilled from phosphorus pentoxide, CD_2Cl_2 was vacuum-transferred from phosphorus pentoxide, and hexanes (Fisher, mixture of isomers, bp 68.5–69.4 °C) was washed successively with 5% nitric acid in sulfuric acid, water, and saturated aqueous sodium carbonate and then distilled from *n*-butyllithium. Nitrosonium salts were purchased from Ozark Mahoning, Tulsa, OK. The $[SbF_6]^-$ salt was used as received; the $[BF_4]^-$ and $[PF_6]^-$ salts were sublimed at 160 °C, 10^{-4} Torr. Tungsten hexacarbonyl (Pressure Chemical Co.) was sublimed prior to use, while trimethylphosphine, dimethylphenylphosphine and tricyclohexylphosphine (Strem) were used as received. The compounds $LW(CO)_5$ (L = Me_3P, Me_2PhP, Cy_3P) were prepared according to a published procedure.[19] Glassware used with the title compounds was oven-dried overnight at 140 °C and transferred into the glovebox while still hot.

$Me_3P(CO)_3(NO)W(\mu\text{-}F)SbF_5$ (3a). Powdered $[NO][SbF_6]$ (2.12 g, 7.98 mmol) was added in one portion to a rapidly stirred solution of $Me_3PW(CO)_5$ (3.03 g, 7.58 mmol) in 100 mL of CH_2Cl_2. The mixture, which was stirred under a partial vacuum in the glovebox, bubbled vigorously and turned orange; in addition an orange precipitate formed. After 0.5 h, the mixture was filtered and the orange solid washed with 20 mL of CH_2Cl_2. This material (0.46 g)—possibly $[trans\text{-}(Me_3P)W(CO)_4(NO)][SbF_6]$[26,27a]—did not dissolve in additional CH_2Cl_2 and would form in apparently irreproducible quantities. The CH_2Cl_2 solution was stripped to give a light yellow powder, which was washed with 3 × 15 mL portions of hexanes; stripping the hexanes washes yielded 0.2 g of unreacted $Me_3PW(CO)_5$. The product was taken up in 20 mL of CH_2Cl_2, and the solution was filtered through Celite and then treated with 20 mL of CCl_2FCClF_2 to yield an unidentified yellow precipitate. The mixture was cooled to −40 °C for 2 h to complete the precipitation and then filtered. About 50 mL of hexanes was than layered onto the CH_2Cl_2/CCl_2FCClF_2 solution and the mixture kept at −40 °C overnight. The resultant bright yellow crystals were filtered to give 2.85 g (66% based on recovered starting material) of **3a**. The supernatant solution was stripped and washed with hexanes to yield 0.25 g of additional product (as a spectroscopically pure powder) and 0.07 g of starting material, for an overall yield of 74% of **3a**: IR (CH_2Cl_2) 2102 (m), 2010 (s), 1690 (s) cm^{-1}; ^1H NMR (CD_2Cl_2) δ 1.80 (d, $^2J_{PH}$ = 9.5 Hz); ^{13}C NMR (CD_2Cl_2, 265 K) 201.45 (d of septets, $^2J_{CP}$ = 41.1 Hz, $^2J_{CF}$ = 9.8 ± 1.4 Hz, trans *CO*), 201.41 (d of septets, $^2J_{CP}$ = 7.3 Hz, $^2J_{CF}$ = 11.1 ± 0.5 Hz, cis *CO*), 15.60 (d, $^2J_{CP}$ = 31.8 Hz) ppm; ^{31}P NMR (CD_2Cl_2, 300 K) −16.25 (septet, $^2J_{PF}$ = 39.8 Hz, $^1J_{PW}$ = 283 Hz) ppm; MS (for ^{184}W, ^{121}Sb) *m/e* 581 (M^+ − CO), 553 (M^+ − 2CO), 374 (M^+ − SbF_6), 365 (M^+ − CO − SbF_5, weak), 337 (M^+ − 2CO − SbF_5), 309 (M^+ − 3CO − SbF_5). Anal. Calcd for $C_6H_9NO_4F_6PSbW$: C, 11.82; H, 1.49; N, 2.30; P, 5.08; F, 18.70. Found: C, 11.58; H, 1.65; N, 2.38; P, 5.16; F, 18.47.

$Me_2PhP(CO)_3(NO)W(\mu\text{-}F)SbF_5$ (3b). Powdered $[NO][SbF_6]$ (0.58 g, 2.17 mmol) was added in one portion to a rapidly stirred solution of $Me_2PhPW(CO)_5$ (1.01 g, 2.18 mmol) in 25 mL of CH_2Cl_2. The solution, which was maintained under a partial vacuum, bubbled vigorously and turned orange immediately. After 1 h, the now green solution was concentrated to 10 mL and filtered, and the filtrate was treated with 25 mL of CCl_2FCClF_2 to give an unidentified fine yellow precipitate. The suspension was cooled to −40 °C and then filtered (yielding only a few milligrams of the unidentified material) to give a yellow solution. The solution was then concentrated until a precipitate (**3b**) was observed (ca. 15–20 mL), and then 25 mL of cold hexanes was layered on. The mixture was allowed to stand at −40 °C overnight, after which it was filtered and the solid washed with hexanes, to give 0.96 g (66% yield) of **3b** as bright yellow crystals: IR (CH_2Cl_2) 2102 (m), 2012 (s), 1690 (s) cm^{-1}; ^1H NMR (CD_2Cl_2) δ 7.55–7.59 (m, 5 H), 2.08 d, $^2J_{PH}$ = 8.9 Hz, 6 H); ^{31}P NMR (CD_2Cl_2, rt) −6.59 (br s, J_{PW} = 279.1 Hz) ppm; ^{31}P NMR (CD_2Cl_2, 200 K) −6.74 (d, J_{PF} = 37.84 Hz; J_{PW} = 274.8 Hz) ppm; MS *m/e* 643 (M^+ − CO), 615 (M^+ − 2CO), 436 (M^+ − SbF_6), 427 (M^+ − CO − SbF_5, weak), 399 (M^+ − 2CO − SbF_5), 371 (M^+ − 3CO − SbF_5), 341 (M^+ − 3CO − NO − SbF_5). Anal. Calcd for $C_{11}H_{11}NO_4F_6PSbW$: C, 19.67; H, 1.65; N, 2.09. Found: C, 19.62; H, 1.54; N, 2.04.

$Cy_3P(CO)_3(NO)W(\mu\text{-}F)SbF_5$ (3c). Powdered $[NO][SbF_6]$ (26 mg, 0.099 mmol) was added to a solution of $Cy_3PW(CO)_5$ (50 mg, 0.083 mmol) in 0.25 mL of CH_2Cl_2. Vigorous bubbling was observed, and the reaction mixture was shaken periodically. After 10 min, the brown-green solution was decanted away from an orange precipitate. Addition of 1 mL of hexanes to the solution gave a cloudy yellow suspension, which was allowed to stand overnight at −40 °C. Filtration gave 17 mg (25% yield) of **3c** as large yellow prisms: IR (CH_2Cl_2) 2094 (m), 2010 (s), 1686 (m) cm^{-1}; ^1H NMR (CD_2Cl_2) δ 2.24 (m, 3 H), 1.91 (m, 12 H), 1.79 (m, 3 H), 1.3–1.6 (m, 15 H); ^{31}P NMR (CD_2Cl_2, 298 K) 36.04 (septet, J_{PF} = 27.3 Hz, J_{PW} = 276 Hz) ppm. Anal. Calcd for $C_{21}H_{33}NO_4F_6PSbW$: C, 30.98; H, 4.09; N, 1.72. Found: C, 31.15; H, 4.27; N, 1.56.

$Me_3P(CO)_3(NO)W(\mu\text{-}F)BF_3$ (5). Powdered $[NO][BF_4]$ (70 mg, 0.60 mmol) was added to a rapidly stirred solution of $Me_3PW(CO)_5$ (200 mg, 0.50 mmol) in 10 mL of CH_2Cl_2. No orange solid was observed, and bubbling subsided after 10 min. The green solution was filtered through Celite and the filtrate was reduced under vacuum to a volume of 6 mL and cooled to −40 °C. Hexanes (8 mL precooled to −40 °C) was layered on, and the mixture was allowed to stand at −40 °C for 12 h. The green solution was decanted away from a yellow gel, reduced to 8 mL, and stored at −40 °C for 12 h. Filtration gave 95 mg (41% yield) of **5** as long yellow needles: IR (CH_2Cl_2) 2095 (w), 2015 (s), 1675 (m) cm^{-1}; ^1H NMR (CD_2Cl_2) δ 1.71 (d, $^2J_{PH}$ = 9.4 Hz); ^{13}C NMR (CD_2Cl_2, 183 K) 201.37 (d of multiplets, $^2J_{CP}$ = 41.2 Hz, $\nu_{1/2} \approx {}^2J_{CF} \approx$ 11 Hz, trans *CO*), 200.96 (d of multiplets, $^2J_{CP}$ = 7 Hz, $\nu_{1/2} \approx {}^2J_{CF} \approx$ 11 Hz, cis *CO*), 14.84 (d, $^2J_{CP}$ = 31.8 Hz) ppm; ^{31}P NMR (CD_2Cl_2, 300 K) −17.46 (quintet, $^2J_{PF}$ = 39.7 Hz, $^1J_{PW}$ = 282 Hz) ppm; ^{19}F NMR (CD_2Cl_2, 185 K) −153.65 (dd, $^2J_{FF}$ = 94.8 Hz, "*J*" = 7.3 Hz, $(\mu\text{-}F)^{10}BF_3$), −153.71 (dd, $^2J_{FF}$ = 95.0 Hz, "*J*" = 6.2 Hz, $(\mu\text{-}F)^{11}BF_3$), −240.52 (qd, $^2J_{FF}$ = 95.4 ± 0.7 Hz, $^2J_{PF}$ = 36.3 ± 1.1 Hz, $(\mu\text{-}F)BF_3$), −145.98 (br s), −148.71 (br s, free $[BF_4]^-$) ppm. Anal. Calcd for $BC_6H_9NO_4F_4PW$: C, 15.64; H, 1.97; N, 3.04. Found: C, 15.37; H, 2.06; N, 2.95.

$Me_3P(CO)_3(NO)W(\mu\text{-}F)PF_5$ (6). Powdered $[NO][PF_6]$ (105 mg, 0.60 mmol) was added to a rapidly stirred solution of $Me_3PW(CO)_5$ (200 mg, 0.50 mmol) in 4 mL of CH_2Cl_2. Slow bubbling and formation of an orange precipitate were observed. After 10 min the yellow solution was filtered through Celite and the filtrate cooled to −40 °C; 6 mL of hexanes (precooled to −40 °C) was layered on and the mixture allowed to stand at −40 °C overnight. The yellow solution was decanted away from a yellow oil, reduced to 7 mL, and stored at −40 °C for 8 h. The product was filtered and washed with 0.5 mL of hexanes to give 56 mg (22% yield) of **6** as yellow needles: IR (CH_2Cl_2) 2100 (m), 2010 (s), 1695 (s); ^1H NMR (CD_2Cl_2) δ 1.79 (d, $^2J_{PH}$ = 9.2 Hz); ^{31}P NMR (CD_2Cl_2, 290 K) −16.64 (septet, $^2J_{PF}$ = 43.9 Hz, $^1J_{PW}$ = 283 Hz, 1 P, PMe_3), −17.35 (d, *J* = 35.4 Hz; impurity that is ~10% of **6**, possibly $Me_3P(CO)_3(NO)WF$), −139.3 (septet, $^1J_{PF}$ = 731.7 Hz, 1 P, bound $[PF_6]^-$), −143.9 (br septet, $^1J_{PF}$ = 711 Hz, 0.3 P, free $[PF_6]^-$) ppm; ^{19}F NMR (CD_2Cl_2, 185 K) −69.60 (dd, $^2J_{FF}$ = 61.4 ± 1.0 Hz, $^1J_{PF}$ = 780.0 Hz, 4 F, $(\mu\text{-}F)P(F_{eq})_4F_{ax}$), −85.30 (d of quintets, $^2J_{FF}$ = 63.6 ± 1.9 Hz, $^1J_{PF}$ = 764.0 Hz, 1 F, $(\mu\text{-}F)P(F_{eq})_4F_{ax}$), −163.99 (d, $^1J_{PF}$ = 496.9 Hz, 1 F, $(\mu\text{-}F)P(F_{eq})_4F_{ax}$), −71.24 (d, $^1J_{PF}$ = 710.3 Hz, 2.5 F, "free" $[PF_6]^-$), −84.09 (d, $^1J_{PF}$ = 971.4 Hz, 0.026 F), −86.21 (br d, $^1J_{PF}$ = 1055.7 Hz, 0.07 F), −86.44 (d, $^1J_{PF}$ = 1072.8 Hz, 0.05 F) ppm. No analysis was attempted due to rapid (ca. 1–2 days) decomposition at room temperature.

[*mer*-(*cis*-Me_3P)(*trans*-CH_3CN)$W(CO)_3(NO)$][PF_6] (7). Powdered $[NO][PF_6]$ (156 mg, 0.90 mmol) was added to a solution of $Me_3PW(CO)_5$ (300 mg, 0.75 mmol) in 15 mL of CH_2Cl_2. The reaction mixture was stirred for 30 min and then filtered through a coarse fritted glass funnel. Acetonitrile (23.4 μL, 0.45 mmol) in 15 mL of CH_2Cl_2 was

Table X. Crystal and Data Collection Parameters[a]

	3b	3c	5	6
formula	$C_{11}H_{11}NO_4F_6PSbW$	$C_{21}H_{33}NO_4F_6PSbW$	$BC_6H_9NO_4F_4PW$	$C_6H_9NO_4F_6P_2W$
fw	671.78	814.06	460.77	518.93
space group	$P2_1/n$	$P\bar{1}$	$P2_1/n$	$P2_1/n$
a, Å	8.838 (3)	9.925 (2)	6.709 (1)	7.424 (2)
b, Å	8.267 (2)	10.604 (2)	12.249 (2)	21.207 (6)
c, Å	25.004 (7)	14.010 (2)	16.457 (3)	9.089 (2)
α, deg		84.088 (3)		
β, deg	94.71 (1)	70.390 (3)	98.352 (7)	99.220 (7)
γ, deg		81.051 (4)		
V, Å^3	1827.33	1371.03	1344.00	1423.45
Z	4	2	4	4
ρ(calc), g cm^{-3}	2.45	1.97	2.29	2.44
abs coeff (μ) cm^{-1}	81.01	54.01	89.85	86.52
transmission factors	0.152–0.236	0.435–0.519	0.384–0.524	0.185–0.701
R	0.056	0.026	0.047	0.061
R_w	0.070	0.035	0.055	0.073

[a] Diffractometer: modified Picker FACS-1. Temperature: −140 °C. Radiation: Mo Kα (λ = 0.7107 Å). Monochromator: graphite. Scan type: $\theta/2\theta$.

added and the solution stirred for 2 h. After the solvent was stripped, the resultant yellow solid was washed with hexanes to remove $Me_3PW(CO)_5$ and recrystallized three times from 2:1 CH_2Cl_2/hexanes to give 110 mg (44% yield) of analytically pure yellow crystals of **7**: IR (CH_2Cl_2) 2274 (w), 2103 (m), 2009 (s), 1706 (s) cm^{-1}; ^{1}H NMR (CD_2Cl_2) δ 2.47 (d, $^5J_{PH}$ = 1.6 Hz, 3 H), 1.83 (d, $^2J_{PH}$ = 9.5 Hz, 9 H); ^{31}P NMR (CD_2Cl_2) −26.80 (s, J_{PW} = 263 Hz, PMe_3), −144.28 (septet, J_{PF} = 710.5 Hz, $[PF_6]^-$) ppm. Anal. Calcd for $C_8H_{12}N_2O_4F_6P_2W$: C, 17.16; H, 2.16; N, 5.00. Found: C, 17.03; H, 2.18; N, 4.86.

***[mer*-(*cis*-Me$_3$P)(*trans*-Me$_3$P)W(CO)$_3$(NO)][SbF$_6$] (8).** Neat PMe_3 (20 mg, 0.26 mmol) was added to a solution of **3a** (104 mg, 0.17 mmol) in 3 mL of CH_2Cl_2, immediately giving a yellow precipitate. The solution was stripped and the bright yellow powder washed with hexanes. The solid was redissolved in 7 mL of CH_2Cl_2, and the mixture was filtered and cooled overnight at −35 °C. After the solid was filtered out and washed with hexanes, 34 mg (29% yield) of **8** was obtained as bright yellow crystals: IR (CH_2Cl_2) 2080 (w), 2002 (s), 1713 (m) cm^{-1}; ^{1}H NMR (CD_2Cl_2) δ 1.87 (d, $^2J_{PH}$ = 9.2 Hz, 9 H), 1.67 (d, $^2J_{PH}$ = 8.6 Hz, 9 H). Anal. Calcd for $C_9H_{18}NO_4F_6P_2SbW$: C, 15.76; H, 2.65; N, 2.04. Found: C, 15.81; H, 2.55;, N, 1.93.

***[mer*-(*cis*-Me$_3$P)(*trans*-Ph$_3$P)(NO)W(CO)$_3$][SbF$_6$] (9).** Triphenylphosphine (86 mg, 0.33 mmol, recrystallized from EtOH) in 1 mL of CH_2Cl_2 was added to a solution of **3a** (200 mg, 0.33 mmol) in 1 mL of CH_2Cl_2 and the yellow solution stirred for 1 h. Hexanes (2 mL) was layered on and the mixture allowed to stand at −40 °C; after 48 h the product was filtered out and washed with cold 50:50 hexanes/CH_2Cl_2. Two recrystallizations with 1:1 CH_2Cl_2/hexanes gave 219 mg (77% yield) of **9** as yellow crystals: IR (CH_2Cl_2) 2090 (w), 2003 (s), 1722 (m) cm^{-1}; ^{1}H NMR (CD_2Cl_2) δ 7.57–7.66 (m, 9 H), 7.37–7.49 (m, 6 H), 1.60 (d, $^2J_{PH}$ = 8.9 Hz, 9 H). Anal. Calcd for $C_{24}H_{24}NO_4F_6P_2SbW$: C, 33.06; H, 2.77; N, 1.61. Found: C, 32.90; H, 2.67; N, 1.62.

***[mer*-(*cis*-Me$_3$P)(*trans*-CH$_3$CN)W(CO)$_3$(NO)][SbF$_6$] (10).** A solution of 14 mg of CH_3CN (0.34 mmol) in 1 mL of CH_2Cl_2 was added in one portion to 103 mg of **3a** (0.17 mmol) in 2 mL of CH_2Cl_2; no visible change in the yellow solution occurred. The solution was immediately pumped to dryness. The solid was taken up in 2 mL of CH_2Cl_2 and the solution filtered and cooled to −40 °C overnight. The product was filtered and washed with hexanes, giving 76 mg (69% yield) of **7** as bright yellow needles: IR (CH_2Cl_2) 2270 (vw), 2102 (m), 2010 (s), 1703 (s) cm^{-1}; ^{1}H NMR (CD_2Cl_2) δ 2.47 (d, $^5J_{PH}$ = 1.8 Hz, 3 H), 1.83 (d, $^2J_{PH}$ = 9.2 Hz, 9 H). Anal. Calcd for $C_8H_{12}N_2O_4F_6PSbW$: C, 14.77; H, 1.86; N, 4.30. Found: C, 14.77; H, 1.79; N, 4.25.

***[mer*-(*cis*-Me$_3$P)(*trans*-CH$_2$CHCHO)W(CO)$_3$(NO)][SbF$_6$] (11).** A solution of acrolein (85 mg, 1.52 mmol) in 0.5 mL of CH_2Cl_2 was added to **3a** (527 mg, 0.86 mmol) in 10 mL of CH_2Cl_2, changing from light to dark yellow. After standing a few minutes, the solution was stripped and the resultant yellow-orange powder taken up in 2 mL of CH_2Cl_2. The mixture was filtered through Celite and the filtrate cooled to −40 °C, and then 3 mL of hexanes was layered on. After standing overnight, the product was filtered and washed with hexanes, giving 537 mg (93% yield) of **11** as large orange crystals: IR (CH_2Cl_2) 2101 (mw), 2015 (s), 1698 (ms), 1635 (m) cm^{-1}; ^{1}H NMR (CD_2Cl_2) δ 9.23 (d, J = 8.5 Hz, 1 H), 7.19 (d, J = 12.6 Hz, 1 H), 7.12 (d, J = 19.7 Hz, 1 H), 6.51 (m, 1 H), 1.79 (d, $^2J_{PH}$ = 9.1 Hz, 9 H); ^{13}C NMR (CD_2Cl_2) 212.49 (br d, J_{PC} = 2.5 Hz, *C*HO, $^1J_{CH}$ = 182.9 Hz, $^{2,3}J_{CH}$ = 18.3, 11.6 Hz), 155.01 (*C*H$_2$, $^1J_{CH}$ = 165.8, 162.1 Hz, $^2J_{CH}$ = 1.1 Hz), 136.57 (*C*H, $^1J_{CH}$ = 169.0 Hz, $^2J_{CH}$ = 18.1, 3.0 Hz) (CH_2*C*HCHO), 200.34 (d, trans J_{PC} = 39.65 Hz, *C*O), 199.72 (d, cis J_{PC} = 7.56 Hz, (*C*O)$_2$), 16.05 (d, J_{PC} = 31.77 Hz, (CH_3)$_3$P) ppm. Anal. Calcd for $C_9H_{13}NO_5F_6PSbW$: C, 16.24; H, 1.97; N, 2.10. Found: C, 15.54; H, 1.91; N, 2.12.

***[mer*-(*cis*-Me$_3$P)(*trans*-camphor)(NO)W(CO)$_3$][SbF$_6$] (12).** (*R*)-(+)-Camphor (25 mg, 0.16 mmol, purified by sublimation) in 1 mL of CH_2Cl_2 was added to a solution of **3a** (100 mg, 0.16 mmol) in 2 mL of CH_2Cl_2 and the yellow solution stirred for 1.25 h. The volume was reduced to 1 mL on a vacuum pump, and 1.5 mL of hexanes was layered on. After standing 2 days at −40 °C, long yellow needles were obtained. Two recrystallizations gave 89 mg (71% yield) of **12**: IR (CH_2Cl_2) 2102 (w), 2013 (s), 1708 (m), 1658 (m); ^{1}H NMR (CD_2Cl_2) δ 2.6 (m, 1 H), 2.5 (m, 1 H), 2.3 (m, 1 H), 1.9–2.2 (m, 2 H), 1.82 (d, $^2J_{PH}$ = 9.2 Hz, 9 H), 1.2–1.6 (m, 2 H), 1.01 (s, 3 H), 0.90 (s, 3 H), 0.80 (s, 3 H). Anal. Calcd for $C_{16}H_{25}NO_5F_6PSbW$: C, 25.22; H, 3.31; N, 1.84. Found: C, 23.85; H, 3.18; N, 1.94.

X-ray Structure Determinations. General Procedure. The title compounds were found to react with epoxy cement. In each case, therefore, a crystal was cut under argon and mounted on a glass fiber in the middle of a small amount of Dow-Corning silicone grease and then immediately transferred to a modified Picker FACS-1 diffractometer where it was kept in a stream of cold (−140 °C) nitrogen.[75] Automatic peak search and centering routines were used for autoindexing and least-squares refinement of the lattice parameters; the number of peaks used for **3b**, **3c**, **5**, and **6** were 23, 25, 24, and 16, respectively. Following data collection, correction for background and Lorentz and polarization effects, space group determination, and (as appropriate) removal of systematically absent and redundant data were carried out; reflections with $I > 3\sigma(I)$ were used to solve the structures. Positions of the tungsten and antimony atoms were obtained from a Patterson synthesis for **3b**. The position of the tungsten atom only was obtained from a Patterson synthesis for **3c** and by using MULTAN for **5** and **6**. All of the remaining non-hydrogen atoms were readily located on electron density and difference electron density maps. Control of the diffractometer and all calculations were carried out on a VAX 11/750 computer using the UCLA crystallographic package, which includes locally edited versions of ABSORB, CARESS, MULTAN, ORFFE, ORFLS, and ORTEP. Scattering factors and corrections for anomalous dispersion for all atoms were taken from ref 76. Further details of the structure determinations are described below, in Table X, and in the supplementary material.

Structure Determination of 3b. Crystals of **3b** were grown at −40 °C by overnight diffusion of precooled hexanes through a fine frit into a concentrated solution of **3b** in ca. 1:1 CH_2Cl_2/CCl_2FCClF_2. The peak shapes observed after centering were relatively broad, and this is undoubtedly responsible for the relatively poor residuals obtained in the final refinement of the structure. Inspection of the data showed that reflections having $0k0$, $k = 2n + 1$, and $h0l$, $h + l = 2n + 1$, were systematically absent, consistent only with space group $P2_1/n$. Positions and isotropic thermal parameters for the 25 non-hydrogen atoms refined (full-matrix least-squares procedure based on F) to a weighted R index of 0.09. An absorption correction was then applied by using an 8 × 8 × 8 grid. Positions for the phenyl hydrogens were calculated (C–H = 1.00 Å), and further refinement with anisotropic thermal parameters for the three heaviest atoms gave R_w = 0.072. Another difference map was used to locate one hydrogen atom on each of the methyl groups, and the

(75) Strouse, C. E. *Rev. Sci. Instrum.* **1976**, *47*, 871–876.
(76) (a) *International Tables for X-ray Crystallography*; Kynoch Press: Birmingham, England, 1974; Vol. IV. (b) Stewart, R. F.; Davidson, E. R.; Simpson, W. T. *J. Chem. Phys.* **1965**, *42*, 3175–3187.

positions of the remaining hydrogen atoms were calculated (P-C-H and H-C-H = 109.5°). Refinement of all non-hydrogen atoms anisotropically resulted in $R_w = 0.068$; this small improvement (for 85 extra variables) combined with the large deviations in the anisotropic thermal parameters indicated that the data were not sufficiently accurate to warrant this degree of refinement. At this point a correction for the 1.5% decay of the three standard reflections was applied, but as expected, the effect was small. Final refinement with anisotropic thermal parameters for tungsten, antimony, and phosphorus only and recalculation of the hydrogen atom positions gave the residuals in Table X. The largest peaks on the final difference map were all due to heavy-atom noise, being randomly oriented about the tungsten and antimony atoms at distances of 1.01-1.21 and 0.96-1.10 Å, respectively. Finally, there is one relatively short intermolecular contact of 2.30 Å between F(6) and H(10) (the hydrogen atom on C(10)).

Structure Determination of 3c. Crystals were obtained by layering hexanes onto a cold solution of **3c** in CH_2Cl_2 and allowing the mixture to stand at -40 °C overnight. The successful solution of the structure ultimately justified the initial assumption of space group $P\bar{1}$. A 1.0% decay in the intensities of the three standard reflections was observed over the course of the data collection, but no correction was applied. Positions and isotropic thermal parameters for the 35 non-hydrogen atoms refined as above to $R_w = 0.076$. Positions for the hydrogen atoms were calculated (C-H = 1.00 Å), and further isotropic refinement gave $R_w = 0.063$. An absorption correction was then applied by using an 8 × 8 × 8 grid. Refinement with anisotropic thermal parameters for all non-hydrogen atoms gave the residuals in Table X. The largest peaks on the final difference map were all due to heavy-atom noise, being randomly oriented about the tungsten and antimony atoms at distances of 0.99-1.10 Å and 1.10-1.16 Å, respectively.

Structure Determination of 5. Crystals of **5** were grown at -40 °C as described above for **3c**. Inspection of the data showed that reflections having $0k0$, $k = 2n + 1$, and $h0l$, $h + l = 2n + 1$, were systematically absent, consistent only with space group $P2_1/n$. A correction for the 3.7% decay of the three standard reflections was applied. Positions and isotropic thermal parameters for the 18 non-hydrogen atoms refined as above to $R_w = 0.062$. An absorption correction was then applied by using an 8 × 8 × 8 grid. Refinement with anisotropic thermal parameters for all non-hydrogen atoms was carried out. A difference map allowed the location of five hydrogen atoms on the three methyl carbons, and the positions of the remaining hydrogen atoms were calculated (P-C-H and H-C-H = 109.5°). Final refinement of all non-hydrogen atoms using anisotropic thermal parameters gave the residuals in Table X. The largest peaks on the final difference map were all due to heavy-atom noise, being randomly oriented about the tungsten atom at distances of 0.97-1.56 Å.

Structure Determination of 6. Crystals of **6** were grown at -40 °C as described above for **3c**. Inspection of the data showed that reflections having $0k0$, $k = 2n + 1$, and $h0l$, $h + l = 2n + 1$, were systematically absent, consistent only with space group $P2_1/n$. A correction for the 2.5% decay of the three standard reflections was applied. Positions and isotropic thermal parameters for the 20 non-hydrogen atoms refined as above to $R_w = 0.103$. An absorption correction was then applied by using an 8 × 8 × 8 grid. Refinement with anisotropic thermal parameters for the three heaviest atoms gave $R_w = 0.078$. A difference map was used to locate one hydrogen atom on each of the methyl groups, and the positions of the remaining hydrogen atoms were then calculated as above. Refinement of all non-hydrogen atoms using anisotropic thermal parameters gave the residuals in Table X. The largest peaks on the final difference map were all due to heavy-atom noise, being randomly oriented about the tungsten atom at distances of 0.09-1.16 Å.

Acknowledgment. We wish to thank Professor C. E. Strouse and Dr. C. B. Knobler for their help with the X-ray structure determinations, Professor K. N. Trueblood for assistance with his thermal motion analysis program, Professor J. W. Faller (Yale University) for helpful discussions, Andrew Fortney for providing a sample of **3b**, and Peter Bonnesen for assistance with several ^{19}F NMR spectra. Financial support was provided by the donors of the Petroleum Research Fund, administered by the American Chemical Society, and by the Chevron Research Co., the UCLA Committee on Research, and a Biomedical Research Support Grant.

Supplementary Material Available: Tables of full crystallographic data for **3b**, **3c**, **5**, and **6**, positional parameters, bond distances and angles, and temperature factors for **3c**, **5**, and **6**, and input frequencies and output force constants for 13 compounds and details of the calculation of the Cotton-Kraihanzel force constants (25 pages); tables of structure factors for **3c**, **5**, and **6** (33 pages). The X-ray data for **3b** is available as supplementary material to ref 15. Ordering information is given on any current masthead page.

Notes

Contribution from Dow Corning Corporation, Midland, Michigan 48686

A New Synthetic Route to Fluorodisilanes via Selective Reduction of Halofluorodisilanes

John J. D'Errico† and Kenneth G. Sharp*

Received September 7, 1988

Our primary interest in fluorodisilanes was as potential molecular precursors to amorphous silicon films[1,2] containing hydrogen and fluorine. The use of fluorodisilanes for this purpose eliminates the need for precursor gas mixtures such as SiF_4/SiH_4.[3] In addition, lower deposition temperatures are required when compared to the case for compounds such as SiF_2H_2.[4]

Several routes to fluorodisilanes have been reported. Mixtures of SiF_2HSiH_3 and SiF_3SiH_3 were generated from the reaction of $SiCl_2HSiH_3$ with SbF_3.[5] Fluorodisilane is obtained via the cleavage of Si-O or Si-N bonds in $(Si_2H_5)_2O$ or $(Si_2H_5)_3N$ by BF_3.[6,7] Also, direct current ("ozonizer") plasma synthesis of the symmetrical disilanes 1,2-difluorodisilane and 1,1,2,2-tetrafluorodisilane via coupling reactions of the radicals derived from the monosilanes SiH_3F and SiH_2F_2 has been reported.[5] This route has the disadvantages of involving slow, low-yield reactions and the difficulty of preparing pure $SiFH_3$.[8]

This report describes the reactions of bromofluoro- or chlorofluorodisilanes with Me_3SnH. These reactions are characterized by the selective reduction of Si-Cl or Si-Br bonds without cleavage of Si-F or Si-Si bonds.

Experimental Section

Materials and Manipulations. All manipulations were conducted by using a recirculating drybox (N_2 atmosphere), Schlenk techniques (Ar atmosphere), and a grease-free glass vacuum line (background pressure $<10^{-4}$ Torr). Trimethyltin chloride, SbF_3, $[(CH_3)_2CHCH_2]_2AlH$ (DIBAL-H, Aldrich Chemical Co.), and VITRIDE (70% $NaAlH_2(OCH_2CH_2OCH_3)_2$ in toluene, Hexcel Specialty Chemicals) were used as obtained. Trimethyltin hydride was prepared from the $LiAlH_4$ reduction

† Present address: Indian Orchard Plant, Monsanto Chemical Co., Springfield, MA 01151.

(1) Stutzmann, M.; Jackson, W. B.; Tsai, C. C. *J. Non-Cryst. Solids* **1985**, *77&78*, 363.
(2) Janai, M.; Weil, R.; Pratt, B. *Phys. Rev. B* **1985**, *31*, 5311.
(3) Uesugi, T.; Hisanori, I.; Matsumura, H. *Jpn. J. Appl. Phys., Part 1* **1985**, *24*, 909.
(4) Sharp, K. G.; D'Errico, J. J. U.S. Patent 4 762 808, Aug 9, 1988.
(5) Drake, J. E.; Westwood, N. P. C. *J. Chem. soc. A* **1971**, 3300.
(6) Abedini, M.; MacDiarmid, A. G. *Inorg. Chem.* **1963**, *2*, 608.
(7) Aylett, B. J. *Adv. Inorg. Chem. Radiochem.* **1968**, *11*, 249.
(8) Ebsworth, E. A. V. *Volatile Silicon Compounds*; Pergamon Press: New York, 1963; p 31.

0020-1669/89/1328-2886$01.50/0